

43p.

(NASA Contract NAS7-100)

N64-17819

CODE-1

(NASA CR-53366;

Technical Report No. 32-544

JPL-TR-32-544)

# Obtaining Free-Flight Dynamic Damping of an Axially Symmetric Body (at All Angles-of-Attack) in a Conventional Wind Tunnel

Peter Jaffe

OTS PRICE  
 XEROX \$ 4.60  
 MICROFILM \$ 1.49

jpl

1304823

JET PROPULSION LABORATORY  
 CALIFORNIA INSTITUTE OF TECHNOLOGY  
 PASADENA, CALIFORNIA


January 15, 1964

43p refs

*Technical Report No. 32-544*

***Obtaining Free-Flight Dynamic Damping of an  
Axially Symmetric Body (at All Angles-of-Attack)  
in a Conventional Wind Tunnel***

*Peter Jaffe*

A handwritten signature in dark ink, reading "R. E. Covey". The signature is written in a cursive style with a horizontal line extending to the right.

R. Covey, Chief  
Aerodynamics Facilities Section

**JET PROPULSION LABORATORY  
CALIFORNIA INSTITUTE OF TECHNOLOGY  
PASADENA, CALIFORNIA**

**January 15, 1964**

Copyright © 1964  
Jet Propulsion Laboratory  
California Institute of Technology

Prepared Under Contract No. NAS 7-100  
National Aeronautics & Space Administration

## CONTENTS

<b>I. Introduction</b>	1
<b>II. Basis of Analysis</b>	5
A. Axes Systems	5
B. Aerodynamic Forces and Moments	5
C. Approach	7
<b>III. General Motion Analysis via Numerical Methods</b>	8
A. General Equations of Motion	8
B. Aerodynamic Forces and Moments	10
C. Angular Rates	10
D. Numerical Integration Procedure	12
E. Discussion of the General Motion Analysis	13
<b>IV. Analytical Solution of Planar Motion</b>	16
A. Planar Motion Equations	16
B. Solution Assuming the Vertical Acceleration is Zero ( $\theta = \alpha$ )	16
C. Nonlinear Versus Linear Pitching Moment	18
D. The Effect of Vertical Motion	22
E. General Planar Solution	24
F. Applications	26
<b>V. Conclusion</b>	35
<b>Nomenclature</b>	36
<b>References</b>	38

## FIGURES

<b>1. Model in free-flight</b>	3
<b>2. Vertical angular position of model shown in Fig. 1</b>	4
<b>3. Axes systems</b>	5
<b>4. General motion axes system</b>	9
<b>5. Offset center-of-mass and velocity diagram</b>	11

# FIGURES (Cont'd)

6. General motion computer program flow diagram . . . . .	14
7. Smooth model release . . . . .	15
8. Center-of-mass offset (0.084 diameters from centerline in yaw plane) . . . . .	15
9. Initial angular velocity in yaw plane ( $\dot{\psi}_0 = 50$ radian/sec) . . . . .	15
10. Ratio of sine designator, $M, r$ , to linear pitching moment slope vs amplitude of oscillation . . . . .	20
11. Ratio of nonlinear to linear angular rates vs the instantaneous angular position for $r = 1$ . . . . .	20
12. Ratio of the linear to nonlinear translational position vs the instantaneous angular position for $r = 1$ . . . . .	21
13. Ratio of nonlinear to linear angular rates vs the instantaneous angular position for $\theta_0 = 90$ deg . . . . .	21
14. Ratio of the linear to nonlinear translational position vs the instantaneous position for $\theta_0 = 90$ deg . . . . .	21
15. Ratio of the nonlinear to linear angular position vs the linear angular position for $\theta_0 = 90$ deg . . . . .	21
16. Pitching moment curves obtained from the Newtonian Impact Theory . . . . .	23
17. Computer motion for hypothetical numerical solution . . . . .	31
18. Perturbated moment curve . . . . .	33

## ABSTRACT

17819 A

Two methods are presented for calculating the dynamic damping parameter,  $C_{m_q} + C_{m_{\dot{\alpha}}}$ , from a novel wind tunnel free-flight technique being developed at the Jet Propulsion Laboratory (JPL). The two methods, which are applicable to nonlinear, high angle-of-attack motion, are: (a) a computer method for nonplanar, nonsymmetrical motion requiring iterations, and (b) a noncomputer solution applicable when the model exhibits planar motion. Both methods assume that the static aerodynamic coefficients are known. The basic hypothesis of the planar solution is that the second-order effects can be determined by assuming that the instantaneous oscillatory frequency is a function of a nonlinear pitching moment of the form  $M \sin(k\alpha)$ . Both methods are applied to representative problems, and solutions using the planar method are compared with results from the computer program.

Author

## I. INTRODUCTION

The aerodynamic forces acting on a body can be separated into two groups: static forces, dependent only upon the angle-of-attack, and forces resulting from the pitching velocity and vertical acceleration (Ref. 1). The contribution of the forces due to motion to the total aerodynamic forces is, generally, quite small. However, their effect on the total motion is greatly magnified if the body is in a negative dynamic pressure gradient ( $dq/dt < 0$ ). An important example of this effect occurs when a vehicle enters a planetary atmosphere. During the first phase of entry, the vehicle experiences an increasing dynamic pressure gradient which continually strengthens the aerodynamic static restoring moment (causing a decrease in the amplitude of oscillation). When the vehicle speed has decreased to about 0.6 of the initial velocity, a reversal occurs, and the vehicle is influenced by a decreasing dynamic pressure gradient. The static restoring moment becomes weaker with each cycle of oscillation and, if it were the only restoring

moment acting, the amplitude of oscillation would increase in order to balance the energies. It is during this phase of entry that the stability derivatives due to the pitching velocity and vertical acceleration have a disproportionately large effect on the amplitude of oscillation (Refs. 2 and 3).

At the present time, these stability derivatives are experimentally obtained either by firing models in a ballistic range or using bearing-mounted and flexure-mounted forced and freely oscillating models in a wind tunnel. The range technique is limited to small angles-of-attack because of model launch problems and the assumptions of linearity in the data analysis. Also, for the blunt-type re-entry bodies, which intrinsically have small stability derivatives due to motion, the resultant accuracies are about the size of the derivatives. The wind tunnel technique of supporting the model on a bearing or flexure yields questionable results below Mach 3. Tests have shown that at the

lower Mach numbers, the sting as well as the base can influence the damping; consequently, the presence of a sting casts suspicion upon the data. In general, the effect of the sting on damping data appears to diminish above Mach 3. However, this must be verified for each configuration before the influence can be neglected. The flexure-mounted technique yields the damping at a particular angle-of-attack as the model oscillates through a very small angular excursion from the mean value. The validity of using this type of data for a body oscillating through a large angle-of-attack range (large perturbations) is questionable, since the flexure data is the result of small perturbations. The bearing technique can duplicate the larger amplitudes of oscillation, but model construction problems limit the amplitude to about 20 deg. In addition, bearing damping itself must always be considered when this type of apparatus is used.

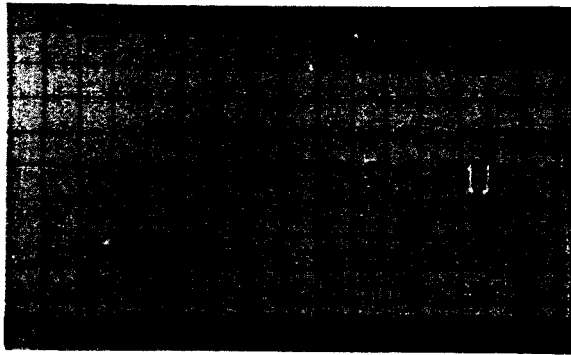
Another technique is currently being developed at JPL which encompasses most of the advantages of both the conventional ballistic range and wind tunnel techniques and retains few of the disadvantages. Briefly, the technique is as follows: Models are suspended on a pre-loaded vertical wire in the wind tunnel at an initial angle-of-attack. After tunnel flow is established, an additional load is applied which ruptures the wire, placing

the model in free-flight<sup>1</sup> (Ref. 4). The motion is recorded by means of a high-speed 35-mm Fastax camera, operating at about 4000 frames/sec, focused on the vertical plane through the tunnel side windows. The prime model motion occurs in a vertical plane parallel to the wind. Motion, as seen in a horizontal plane parallel to the wind, is transcribed simultaneously into the vertical plane by means of a pair of mirrors at the top and bottom of the wind tunnel (each at a 45-deg angle).

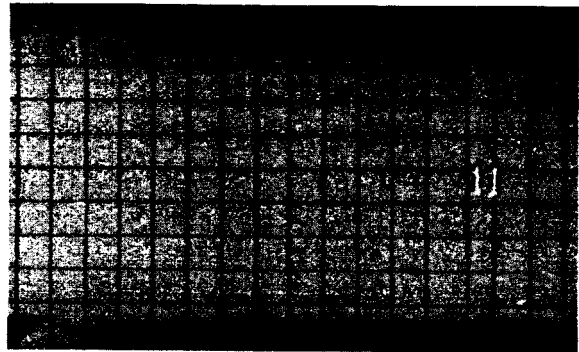
Figure 1 shows a representative sequence of photographs of a model in free-flight. Notice that the horizontal motion is visible in the bottom of each frame and that there is essentially no yawing. From this photographic history, the vertical angular position was determined as a function of time. This is plotted in Fig. 2. It is the purpose of this report to present methods for obtaining the stability derivatives from the motion history data obtained with the wind tunnel free-flight testing technique.

---

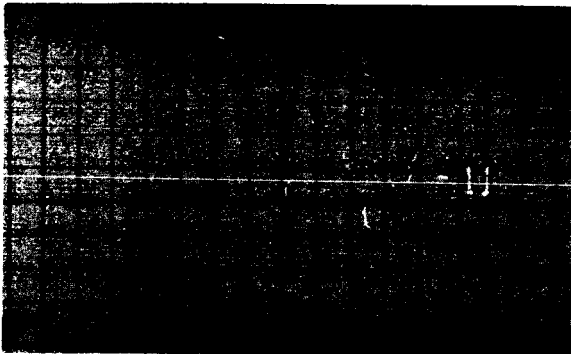
<sup>1</sup>Even before this technique is perfected it is being superseded by a more sophisticated method where the model is launched upstream with a pneumatic gun. By carefully controlling the launch thrust the model can be made to go to the edge of the viewing window and return, yielding twice as much information as the wire release.



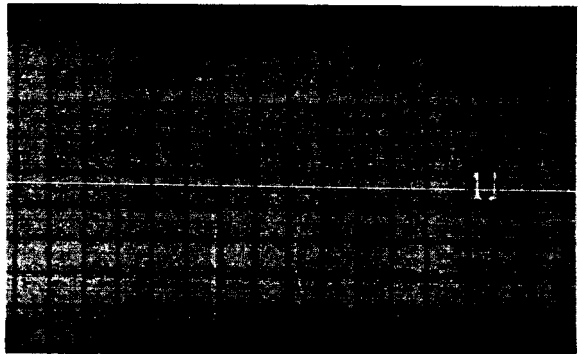
FRAME 116



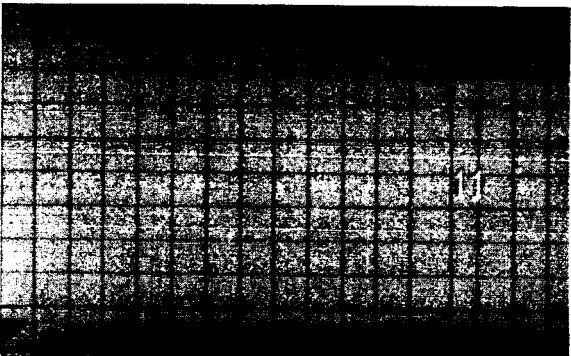
FRAME 122



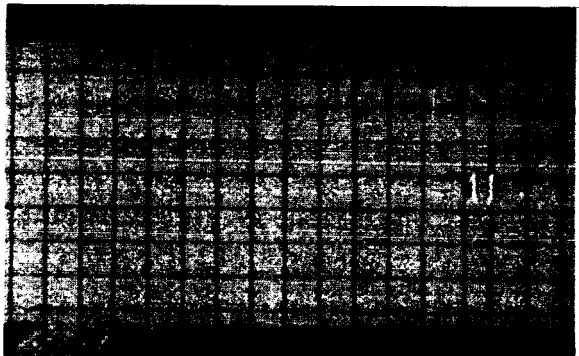
FRAME 118



FRAME 124



FRAME 120



FRAME 126

**Fig. 1. Model in free-flight**

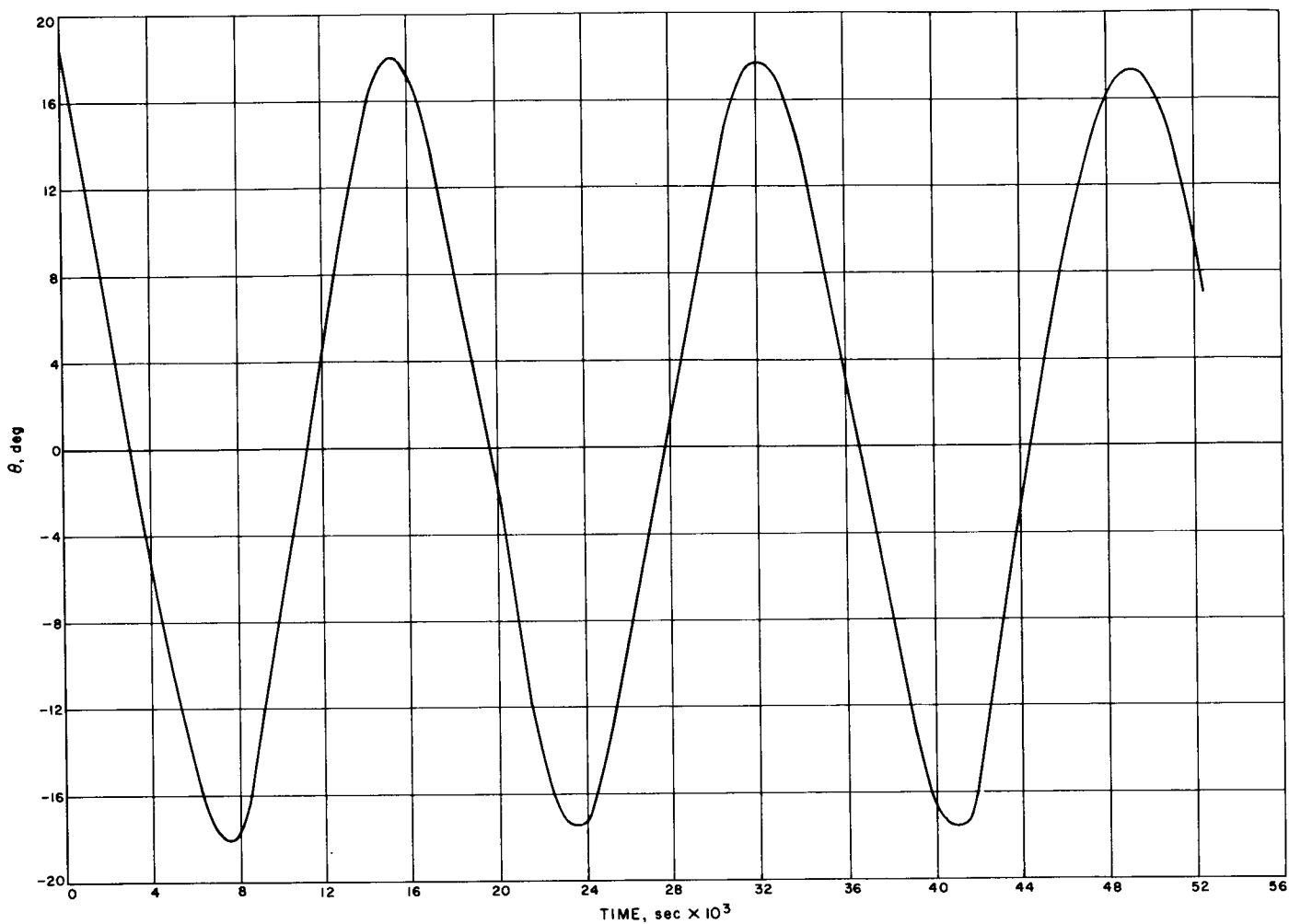


Fig. 2. Vertical angular position of model shown in Fig. 1

## II. BASIS OF ANALYSIS

### A. Axes Systems

The sequence of photographs in Fig. 1 describes the motion of the model with respect to a tunnel-fixed axes system  $\tilde{X}_T, \tilde{Y}_T, \tilde{Z}_T$ , which is essentially an inertial system. This system, however, is not well suited for analysis; instead, a medium-fixed system will be the basis for all further development. Let  $\tilde{X}, \tilde{Y}, \tilde{Z}$  be a set of Cartesian coordinates parallel to  $\tilde{X}_T, \tilde{Y}_T, \tilde{Z}_T$  and traveling parallel to the tunnel centerline at rate  $V_\infty$ .<sup>2</sup>  $\tilde{X}$  is parallel to the tunnel centerline, toward the oncoming wind.  $\tilde{Y}$  and  $\tilde{Z}$  are to the right and down, respectively (see Fig. 3).  $X, Y, Z$  will denote the position of the model center-of-mass with respect to this system, and  $\hat{X}, \hat{Y}, \hat{Z}$  will denote unit vectors in the  $\tilde{X}, \tilde{Y}, \tilde{Z}$  directions. A parallel system  $X_m, Y_m, Z_m$ , fixed at the model center-of-mass will also be employed. At time zero, the three axes systems are defined as having the same origin, therefore, if  $X_T$  is the position of the model center-of-mass with respect to inertial space,  $X_T = V_\infty t - X$ . This transformation to a medium fixed velocity reference is necessary since aerodynamic forces are functions of the angle-of-attack<sup>3</sup> and dynamic pressure,  $q = \frac{1}{2} \rho V^2$ , both of which are based on the relative velocity between the medium and model.

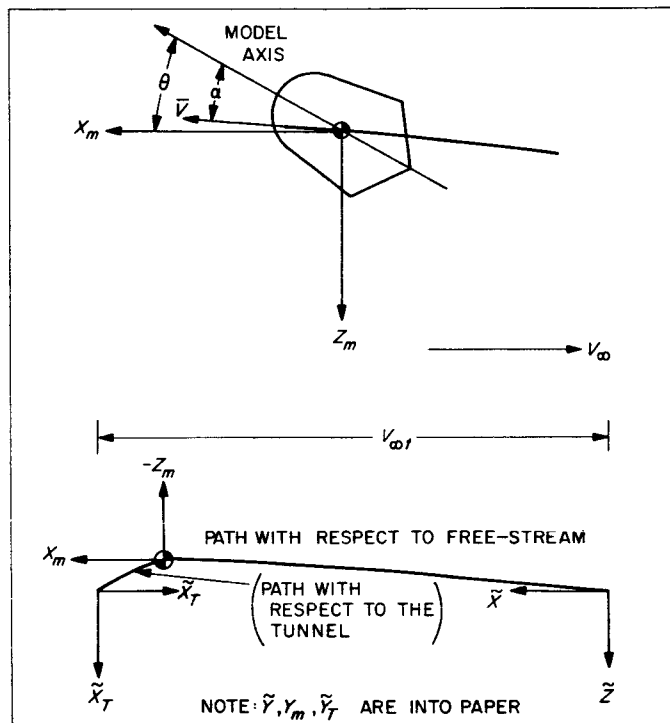


Fig. 3. Axes systems

### B. Aerodynamic Forces and Moments

According to the first-order linear theory, a body exhibiting XZ planar motion will be acted upon by the following aerodynamic forces and moments:

$$F_{X_m} = q A C_{x_0}$$

$$F_{Z_m} = q A \left[ \frac{\partial C_z}{\partial \alpha} \right]_{\alpha \rightarrow 0} \alpha + q A \left[ \frac{\partial C_z}{\partial \left( \frac{\dot{\theta} d}{V} \right)} \right]_{\dot{\theta} \rightarrow 0} \left( \frac{\dot{\theta} d}{V} \right) + q A \left[ \frac{\partial C_z}{\partial \left( \frac{\dot{\alpha} d}{V} \right)} \right]_{\dot{\alpha} \rightarrow 0} \left( \frac{\dot{\alpha} d}{V} \right)$$

$$M_{Y_m} = q A d \left[ \frac{\partial C_m}{\partial \alpha} \right]_{\alpha \rightarrow 0} \alpha + q A d \left[ \frac{\partial C_m}{\partial \left( \frac{\dot{\theta} d}{V} \right)} \right]_{\dot{\theta} \rightarrow 0} \left( \frac{\dot{\theta} d}{V} \right) + q A d \left[ \frac{\partial C_m}{\partial \left( \frac{\dot{\alpha} d}{V} \right)} \right]_{\dot{\alpha} \rightarrow 0} \left( \frac{\dot{\alpha} d}{V} \right)$$

<sup>2</sup> $V_\infty$  is the steady flow velocity in the wind tunnel and is therefore constant.

<sup>3</sup>The angle-of-attack is defined as the angle between the relative velocity vector and the model centerline.

In these equations, all coefficients of  $\alpha$ ,  $\dot{\alpha}d/V$ , and  $\dot{\theta}d/V$  are constant. The nature of the stability derivatives due to  $\dot{\alpha}$  and  $\dot{\theta}$  are now considered. If a body is constrained so that the acceleration in the Z direction is zero then  $\alpha = \theta$  and  $\dot{\alpha} = \dot{\theta}$ . On the other hand, if the body is constrained in  $\theta$ , as in the case of a plunging body, the  $\theta$  time-derivatives will be zero (Ref. 1). It follows that for bodies traveling at high velocities and oscillating rapidly,<sup>4</sup> which is the situation being considered,  $\dot{\alpha} \cong \dot{\theta}$ .<sup>5</sup> Employing this qualification, the moment equation and Z force equations can be written as follows:

$$F_{z_m} = q A \left[ \frac{\partial C_z}{\partial \alpha} \right]_{\dot{\alpha} \rightarrow 0} \alpha + q A \left\{ \left[ \frac{\partial C_z}{\partial \left( \frac{\dot{\theta}d}{V} \right)} \right]_{\dot{\theta} \rightarrow 0} + \left[ \frac{\partial C_z}{\partial \left( \frac{\dot{\alpha}d}{V} \right)} \right]_{\dot{\alpha} \rightarrow 0} \right\} \left( \frac{\dot{\theta}d}{V} \right)$$

$$F_{y_m} = q A d \left[ \frac{\partial C_m}{\partial \alpha} \right]_{\dot{\alpha} \rightarrow 0} \alpha + q A d \left\{ \left[ \frac{\partial C_m}{\partial \left( \frac{\dot{\theta}d}{V} \right)} \right]_{\dot{\theta} \rightarrow 0} + \left[ \frac{\partial C_m}{\partial \left( \frac{\dot{\alpha}d}{V} \right)} \right]_{\dot{\alpha} \rightarrow 0} \right\} \left( \frac{\dot{\theta}d}{V} \right)$$

Also, as shall be shown later, the force,  $F_z$ , has only a second-order effect on the amplitude of oscillation; only a negligible error will result if the coefficient of  $\theta$  in this equation is neglected.

Since the analysis to be presented will not be limited to small disturbances, where only the linear approach is applicable, the previously described force equations are inadequate and a more general set must be employed. Coupling the preceding discussion with what experience has shown to be the aerodynamic forces and moments of measurable consequence, the following set will be used in the analytical development:

$$F_{x_m} = - q A C_x$$

$$F_{z_m} = - q A C_z$$

$$M_{y_m} = q A d C_m + q A d \overline{C_{m_q}} \left( \frac{\dot{\theta}d}{V} \right)$$

<sup>4</sup>In the sequence of Fig. 1, the frequency of oscillation is about 60 cps and  $V \approx 2,300$  ft/sec.

<sup>5</sup>Considering first-order effects  $\dot{\alpha} = \dot{\theta} - \frac{qA}{mV} \left[ \frac{\partial C_z}{\partial \alpha} \right] \theta$  and  $\theta = \theta_0 \cos(\omega t)$ , therefore

$\alpha = -\theta_0 \omega \sin(\omega t) - \frac{qA}{mV} \left[ \frac{\partial C_z}{\partial \alpha} \right] \theta_0 \cos(\omega t)$ . Typically  $\omega$  is in the order of 250 radians/sec

and  $\frac{qA}{m} \left[ \frac{\partial C_z}{\partial \alpha} \right]$  is in the order of  $2 \times 10^3$  ft/sec<sup>2</sup>. For high velocities the  $\dot{\theta}$  term (first term)

completely dominates the value of  $\dot{\alpha}$  except for a very short interval of time at  $\omega t = n\pi$ . Furthermore, time integrating the  $\dot{\alpha}$  equation over a cycle of motion for the case when  $V = 10^3$  ft/sec, indicates that the  $\dot{\theta}$  term contributes better than 99 percent of the total.

$C_x$ ,  $C_z$  and  $C_m$  are functions of the angle-of-attack;  $\overline{C_{m_q}}$  is the effective constant value of

$$\left\{ \left[ \frac{\partial C_m}{\partial \left( \frac{\dot{\theta} d}{V} \right)} \right]_{\dot{\theta} \rightarrow 0} + \left[ \frac{\partial C_m}{\partial \left( \frac{\dot{\alpha} d}{V} \right)} \right]_{\dot{\alpha} \rightarrow 0} \right\}$$

### C. Approach

The criterion in designing the model and subsequently releasing it in free-flight is to obtain planar, vertical motion. The model's constraining wire passes through the model axis at some initial angle-of-attack. The wire hole is several thousandths of an inch greater than the wire; the model is prevented from sliding up and down by a pair of lugs. When flow is established, it tends to align and stabilize these axially symmetric models in the XZ plane. During a normal release this alignment is usually main-

tained; however, the process of releasing the model may contribute initial angular and translational velocities. In addition, when the model's center-of-mass does not lie on the model axis, nonplanar or nonsymmetrical motion will result. This report will present two solutions to the proposed problem: (1) a detailed solution of the planar motion case and (2) a general solution which must, by its very nature, be an all encompassing computer-type solution capable of accommodating all kinds of misalignments and initial velocities.

### III. GENERAL MOTION ANALYSIS VIA NUMERICAL METHODS

To determine  $\overline{C_{mq}}$ , in the general case, the motion of the model is calculated with a solution of the complete six-degree-of-freedom equations of motion, via numerical methods. This solution requires that the static aerodynamic coefficients  $C_A$ ,  $C_N$ ,  $C_m$  be known. This Section is a formulation of these equations and their extension to a computer program.

#### A. General Equations of Motion

Figure 4 shows the model in three-dimensional space.  $X_m, Y_m, Z_m$  is again a Cartesian axes system fixed at the model center-of-mass, moving parallel to the medium-fixed system  $\tilde{X}, \tilde{Y}, \tilde{Z}$ , and the inertial system  $\tilde{X}_T, \tilde{Y}_T, \tilde{Z}_T$ . Angles  $\psi$ ,  $\theta$ , and  $\phi$  are Euler angles,  $e_1, e_2, e_3$  are orthogonal body axes whose origin is the center-of-mass.  $\hat{e}_1, \hat{e}_2, \hat{e}_3$  are the corresponding unit vectors. Since system  $X_m, Y_m, Z_m$  is parallel to the inertial system, the following transformation, describing the angular motion of the body in terms of inertial axes, can be written.

$$\begin{bmatrix} X_m \\ Y_m \\ Z_m \end{bmatrix} = \begin{bmatrix} \cos \theta \sin \psi & \sin \theta \cos \psi \sin \phi - \sin \psi \cos \phi & \sin \theta \cos \psi \cos \phi + \sin \psi \sin \phi \\ \cos \theta \sin \psi & \sin \theta \sin \psi \sin \phi + \cos \psi \cos \phi & \sin \theta \sin \psi \cos \phi - \cos \psi \sin \phi \\ -\sin \theta & \cos \theta \sin \phi & \cos \theta \cos \phi \end{bmatrix} \begin{bmatrix} e_1 \\ e_2 \\ e_3 \end{bmatrix}$$

This matrix will be denoted  $[A^{-1}]$ , i.e.,  $[e] = [A] [X_m]$ ; it should be noted that this is an orthogonal transformation, therefore,  $[A^{-1}] = [A^T]$ .

The translational motion of the center-of-mass with respect to the medium is given by the following equations:

$$\bar{R} = X \hat{X} + Y \hat{Y} + Z \hat{Z}$$

$$\dot{\bar{R}} = \dot{X} \hat{X} + \dot{Y} \hat{Y} + \dot{Z} \hat{Z}$$

$$\ddot{\bar{R}} = \ddot{X} \hat{X} + \ddot{Y} \hat{Y} + \ddot{Z} \hat{Z}$$

Note that the acceleration,  $\bar{R}$ , with respect to the medium is the acceleration with respect to inertial space since  $V_\infty$  is a constant.

The total angular velocity of the model with respect to inertial space is

$$\bar{\omega} = \omega_1 \hat{e}_1 + \omega_2 \hat{e}_2 + \omega_3 \hat{e}_3$$

$$\begin{aligned} \bar{\omega} = & (\dot{\phi} - \dot{\psi} \sin \theta) e_1 + (\dot{\theta} \cos \phi + \dot{\psi} \cos \theta \sin \phi) \hat{e}_2 \\ & + (\dot{\psi} \cos \theta \cos \phi - \dot{\theta} \sin \phi) \hat{e}_3 \end{aligned}$$

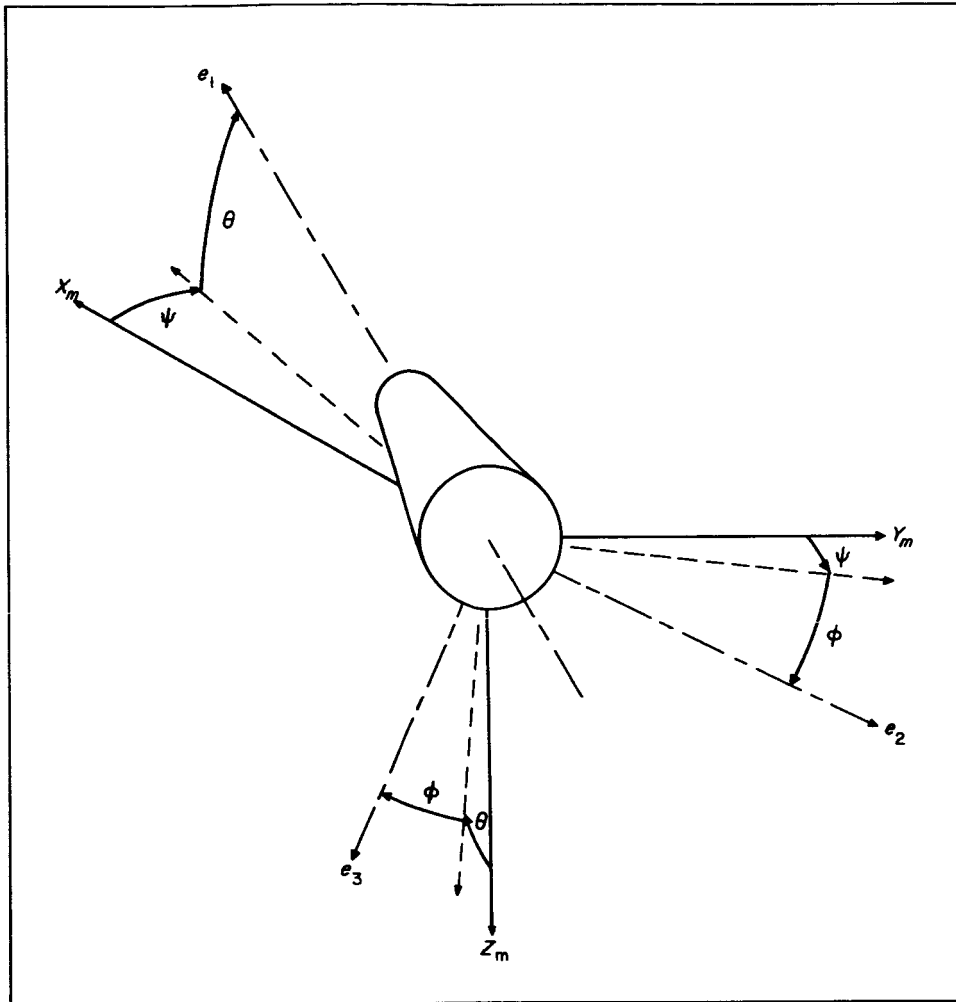


Fig. 4. General motion axes system

Assuming that the principal axes are coincident with the body axes, the angular momentum and angular accelerations are

$$\begin{aligned}\bar{h} &= I_1 \omega_1 \hat{e}_1 + I_2 \omega_2 \hat{e}_2 + I_3 \omega_3 \hat{e}_3 \\ \dot{\bar{h}} &= \{I_1 \dot{\omega}_1 + \omega_2 \omega_3 (I_3 - I_2)\} \hat{e}_1 + \{I_2 \dot{\omega}_2 + \omega_1 \omega_3 (I_1 - I_3)\} \hat{e}_2 \\ &\quad + \{I_3 \dot{\omega}_3 + \omega_1 \omega_2 (I_2 - I_1)\} \hat{e}_3\end{aligned}$$

A small error will result in the solution for those cases when the center-of-mass is offset from the model centerline. However, since these offsets are practically only aberrations of small magnitude, the error produced by the cross product quantities will be negligible.<sup>6</sup> The effect of the offset will not be neglected for the moment calculations later.

<sup>6</sup>In severe cases, this error could be eliminated by including the cross product terms; this would increase the complexity of the integration routine.

From the velocity equation and matrix  $[A]$  a set of body axes velocities  $u_1$ ,  $u_2$ , and  $u_3$  at the center-of-mass can be obtained. Letting  $r$  be the center-of-mass offset with respect to the body, the velocity at the geometric centroid can be calculated (see Fig. 5):

$$\bar{V}_c = \bar{V}_{c.m.} + \bar{\omega} \times \bar{r}$$

$$\bar{V}_c = (u_1 + \omega_2 \varepsilon_3 - \omega_3 \varepsilon_2) \hat{e}_1 + (u_2 - \omega_1 \varepsilon_3) \hat{e}_2 + (u_3 + \omega_1 \varepsilon_2) \hat{e}_3$$

$$\bar{V}_c = v_1 \hat{e}_1 + v_2 \hat{e}_2 + v_3 \hat{e}_3$$

Knowing the velocity at the geometric centroid the angles relating the model centerline with the velocity vector can then be determined

$$\eta = \tan^{-1} \frac{\sqrt{v_2^2 + v_3^2}}{v_1} = \text{total angle-of-attack}$$

$$\alpha = \tan^{-1} \frac{v_3}{v_1} = \text{vertical plane angle-of-attack}$$

$$\beta = \tan^{-1} \frac{v_2}{v_1} = \text{angle of side-slip}$$

## B. Aerodynamic Forces and Moments

The static aerodynamic forces and moments are functions of  $C_A$ ,  $C_N$ , and the c.p., which in turn are functions of  $\eta$  (see Fig. 5). In addition, since the analysis is restricted to axially symmetric bodies, the forces act through the geometric centerline and the total angle-of-attack and dynamic pressure are based upon the model velocity at the centroid.

The aerodynamic driving forces are

$$\bar{F}_1 = -C_A q_c A \hat{e}_1$$

$$\bar{F}_2 = -C_N q_c A \frac{v_2}{\sqrt{v_2^2 + v_3^2}} \hat{e}_2$$

$$\bar{F}_3 = -C_N q_c A \frac{v_3}{\sqrt{v_2^2 + v_3^2}} \hat{e}_3$$

These forces and moments are converted to the inertial system by matrix  $[A^{-1}]$ ; a gravitational force in the Z direction is then added.

## C. Angular Rates

$$\omega_1 = \dot{\phi} - \dot{\psi} \sin \theta$$

$$\omega_2 = \dot{\theta} \cos \phi + \dot{\psi} \cos \theta \sin \phi$$

$$\omega_3 = -\dot{\theta} \sin \phi + \dot{\psi} \cos \theta \cos \phi$$

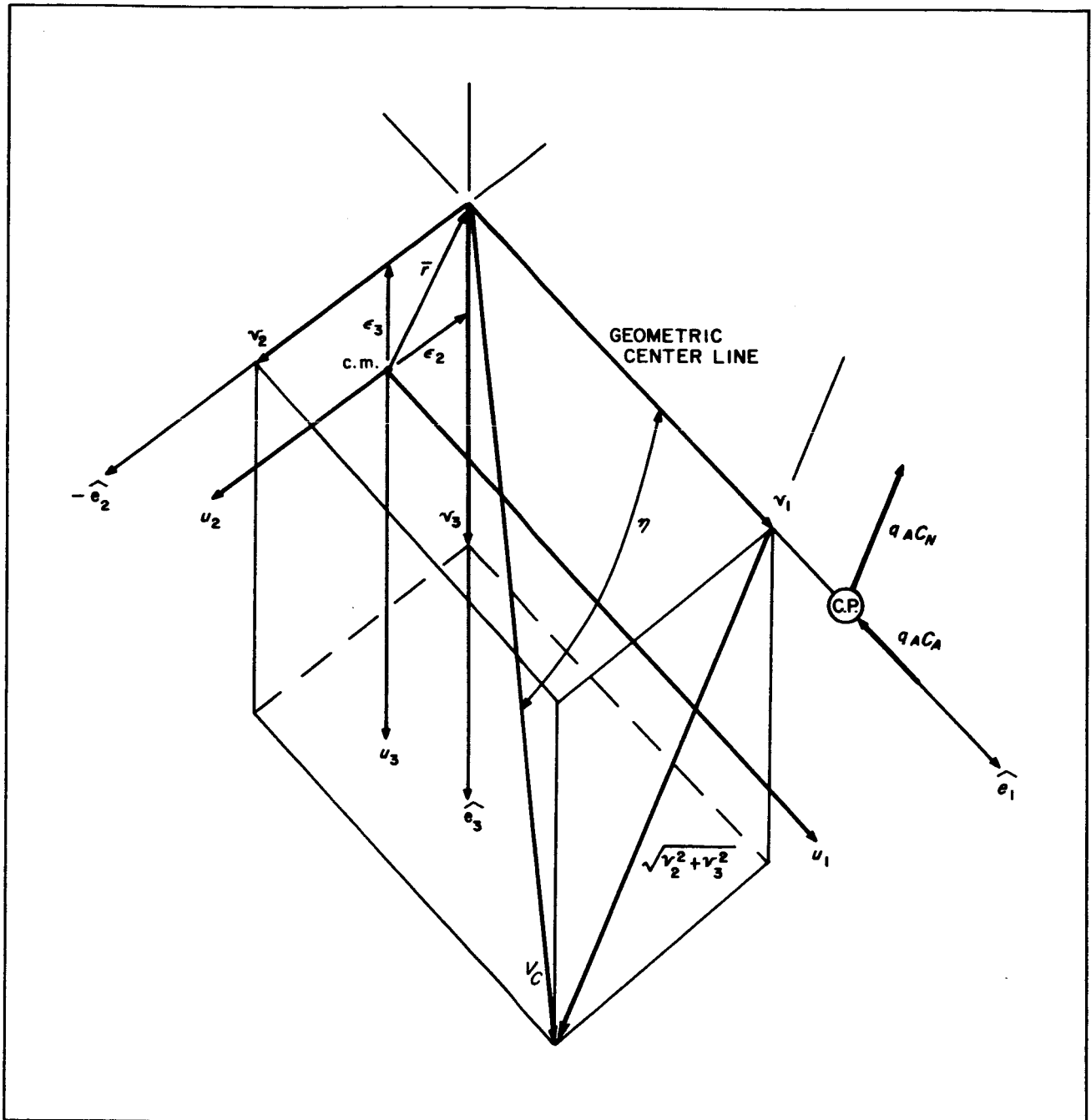


Fig. 5. Offset center-of-mass and velocity diagram

or in matrix form:

$$\begin{bmatrix} \omega_1 \\ \omega_2 \\ \omega_3 \end{bmatrix} = \begin{bmatrix} \sin \theta & 0 & 1 \\ \cos \theta \sin \phi & \cos \phi & 0 \\ \cos \theta \cos \phi & -\sin \phi & 0 \end{bmatrix} \begin{bmatrix} \dot{\psi} \\ \dot{\theta} \\ \dot{\phi} \end{bmatrix}$$

The moments are

$$\overline{M}_1 = (F_2 \varepsilon_3 - F_3 \varepsilon_2) \hat{e}_1$$

$$\overline{M}_2 = \{F_3 (\text{c.p.} - \text{c.m.}) - F_1 \varepsilon_3 + M_{2D}\} \hat{e}_2$$

$$\overline{M}_3 = \{-F_2 (\text{c.p.} - \text{c.m.}) + F_1 \varepsilon_2 + M_{3D}\} \hat{e}_3$$

where the  $M_D$  terms are

$$M_{2D} = \overline{C_{m_{q_2}}} \frac{q A d^2}{V_c} \omega_2$$

$$M_{3D} = \overline{C_{m_{q_3}}} \frac{q A d^2}{V_c} \omega_3$$

$\overline{C_{m_{q_2}}}$  and  $\overline{C_{m_{q_3}}}$  are functions of  $\alpha$  and  $\beta$ , respectively.

The inverse transformation is

$$\begin{bmatrix} \dot{\psi} \\ \dot{\theta} \\ \dot{\phi} \end{bmatrix} = -\frac{1}{\cos \theta} \begin{bmatrix} 0 & -\sin \phi & \cos \phi \\ 0 & -\cos \theta \sin \phi & \cos \theta \sin \phi \\ -\cos \theta & -\sin \theta \sin \phi & -\sin \theta \cos \phi \end{bmatrix} \begin{bmatrix} \omega_1 \\ \omega_2 \\ \omega_3 \end{bmatrix}$$

This matrix will be denoted  $[B^{-1}]$ .

#### D. Numerical Integration Procedure

The preceding motion equations are solved with a computer by separating time into very small finite intervals,  $\delta t$ , and integrating. As an example, consider the  $M_1$  component of moment,

$$M_1 = I_1 \dot{\omega}_1 + \omega_2 \omega_3 (I_3 - I_2)$$

$$\dot{\omega}_1 = \frac{M_1}{I_1} + \frac{\omega_2 \omega_3}{I_1} (I_3 - I_2)$$

During the short interval of time  $\delta t$ , the terms on the right side of the equation will be considered constant.

Therefore,

$$\int_{(n-1)\delta t}^{n\delta t} d\omega_1 = \dot{\omega}_1 \int_{(n-1)\delta t}^{n\delta t} dt$$

and

$$\omega_{1n\delta t} = \omega_{1(n-1)\delta t} + \delta\omega_1 \text{ where } \delta\omega_1 = \dot{\omega}_1 \delta t$$

Considering all components,

$$\begin{bmatrix} \dot{\psi} \\ \dot{\theta} \\ \dot{\phi} \end{bmatrix} = [B^{-1}] \begin{bmatrix} \omega_1 + \delta\omega_1 \\ \omega_2 + \delta\omega_2 \\ \omega_3 + \delta\omega_3 \end{bmatrix}$$

or

$$\begin{bmatrix} \dot{\psi} \\ \dot{\theta} \\ \dot{\phi} \end{bmatrix}_{n\delta t} = \begin{bmatrix} \dot{\psi} \\ \dot{\theta} \\ \dot{\phi} \end{bmatrix}_{(n-1)\delta t} + [B^{-1}] \begin{bmatrix} \delta\omega_1 \\ \delta\omega_2 \\ \delta\omega_3 \end{bmatrix}$$

Note:

$$[B^{-1}] \begin{bmatrix} \delta\omega_1 \\ \delta\omega_2 \\ \delta\omega_3 \end{bmatrix} = \begin{bmatrix} \delta\dot{\psi} \\ \delta\dot{\theta} \\ \delta\dot{\phi} \end{bmatrix}$$

### E. Discussion of the General Motion Analysis

Figure 6 shows a computer flow diagram which links the previously formulated equations and the integration scheme into a usable general motion computer program. Three examples from the computer analysis are presented here to describe typical free-flight motion. All three examples are for motion of the model shown in Fig. 1, released at  $\theta = 60$  deg. Different initial conditions were used for each example. The static aerodynamic coefficients used in these examples were obtained from wind tunnel tests (Ref. 5); a  $\overline{C}_{m_q}$  value of  $-0.1$  was used in the computations.

In the first example, the center-of-mass lies along the model centerline and the model is released smoothly, as would be the condition if the wire release mechanism did not impart any motion to the model. Figure 7 shows the Euler angle,  $\theta$ , versus the relative distance between the medium and the model,  $X$ . Included on the plot is the angle  $(\theta - \alpha)$ , the difference between the Euler angle and the angle-of-attack, magnified 500 times.

In the second example, at the time of release, the center-of-mass was placed at a position 0.084 base diameters to the right of the centerline (looking forward on the model) on the  $e_1 e_2$  plane ( $\phi = 0$ ). Immediately after placing the model in free-flight, the axial force acting along the geometric centerline causes a moment due to the offset resulting in body motion in the  $e_1 e_2$  plane. Also, the normal force acting at the centerline causes rotational motion about the spin axis,  $e_1$ . The Euler angles,  $\psi$ ,  $\theta$ ,  $\phi$ , versus  $X$  are shown in Fig. 8.

The third example depicts the motion resulting from an initial angular velocity,  $\dot{\psi}$  (50 radians/sec). This could occur if the wire release mechanism did impart some initial velocity. Immediately after wire release the  $\theta$  and  $\psi$  motions are out of phase because, at that time  $\dot{\theta} = 0$ , and  $\dot{\psi}$  has a finite value. As time progresses, there is a coupling of motion and a continual change in the phase relationship. Figure 9 shows the Euler angles versus  $X$  for this example. Notice that the model motions resulting from both the offset center-of-mass and the initial yaw velocity ( $\dot{\psi}$ ) do not pass through the  $X$  axis, i.e.,  $\eta$  is never zero.

The method of obtaining  $\overline{C}_{m_q}$  from the computer analysis is an iterative procedure. First, the motion is determined for  $\overline{C}_{m_q} = 0$ . Estimates of initial conditions required to cause the nonsymmetric motion are made. Using these estimates, the motion is computed and compared with the experimental data. If necessary, new values are tried and this process is continued until reasonable agreement is reached. Then, the motion for several values of  $\overline{C}_{m_q}$  is computed and, subsequently, a correlation between decay per cycle and  $\overline{C}_{m_q}$  is developed. In this manner, the correct  $\overline{C}_{m_q}$ , corresponding to the experimental decay, can be obtained. This procedure is costly and time consuming and, occasionally, the motion is so complex as to defy solution. It is anticipated that the technique for placing the models into free-flight will be advanced to the point where the planar solution, presented in the next Section, will be applicable in most cases.

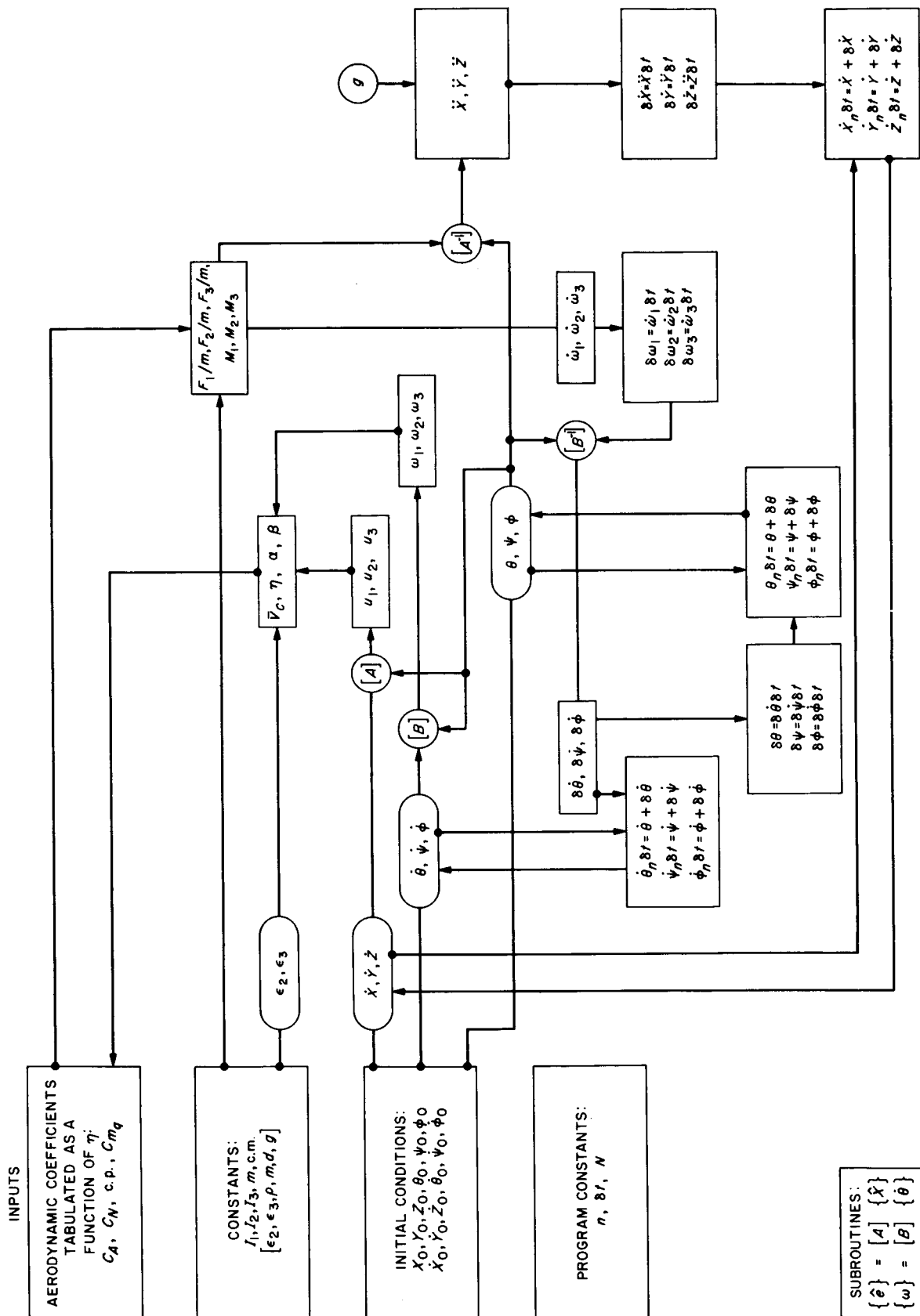


Fig. 6. General motion computer program flow diagram

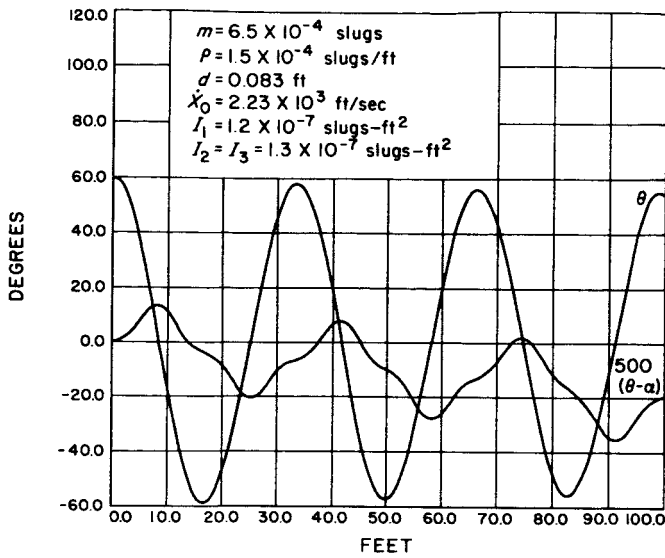


Fig. 7. Smooth model release

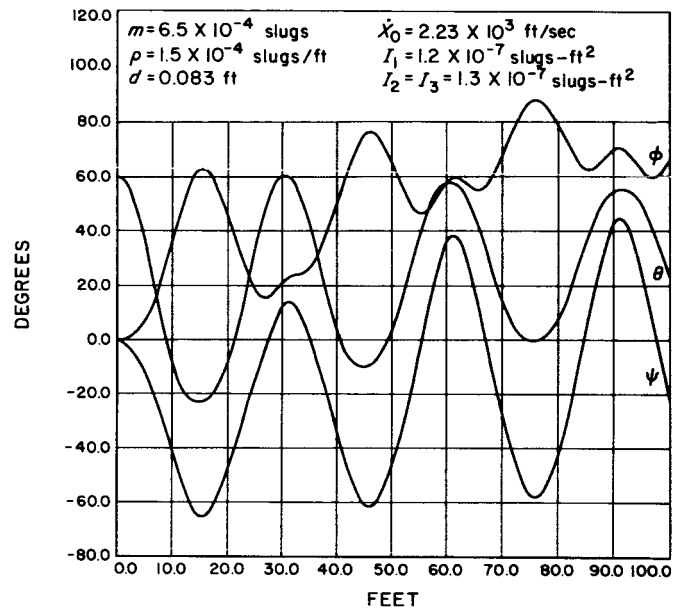
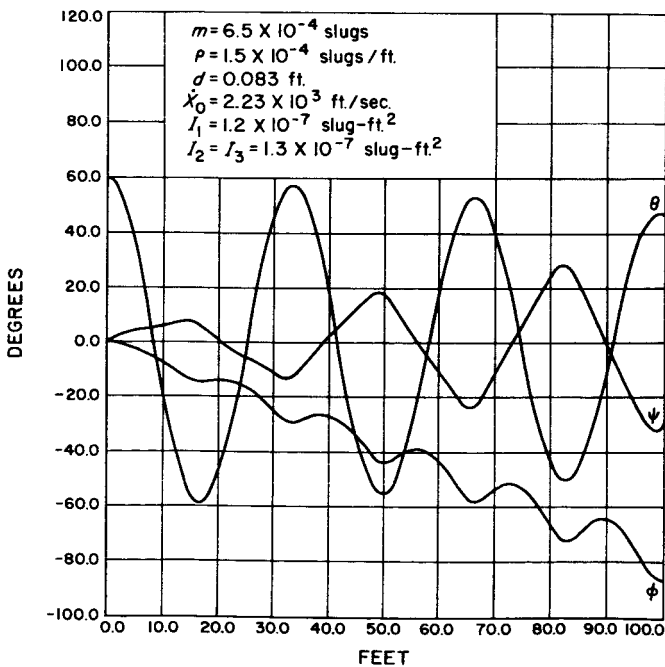


Fig. 8. Center-of-mass offset (0.084 diameters from centerline in yaw plane)

Fig. 9. Initial angular velocity in yaw plane ( $\psi_0 = 50$  radian/sec)

## IV. ANALYTICAL SOLUTION OF PLANAR MOTION

If a model is placed into free-flight without any initial velocities, and its center-of-mass is along the geometric centerline, the resultant motion may be considered planar. In this Section, planar motion will be thoroughly investigated and a non-numerical technique for analyzing the motion will be developed. For simplicity, motion in the XZ plane will be considered (see Fig. 3). The XZ plane is assumed to coincide with the  $X_m Z_m$  plane. At  $t_0 = 0$ , the velocity is  $\bar{V} = V_\infty \hat{X}$ , and the model is at an initial "cock" angle  $\theta_0$ . The model is released at  $t_0$  and, subsequently, at  $t_0 + 0$  it is in flight. The requirement of no initial velocities means that  $\dot{Z}_0$  and  $\dot{Y}_0$  are zero at  $t_0$  and, also, that the angle  $(\alpha - \theta)$  must be zero at  $t_0$ .

### A. Planar Motion Equations

The prime aerodynamic forces<sup>7</sup> acting at the center-of-mass are

$$F_{x_m} = -\frac{1}{2} \rho V^2 A C_x$$

$$F_{z_m} = -\frac{1}{2} \rho V^2 A C_z$$

$$M_{y_m} = \frac{1}{2} \rho V^2 A C_m + \frac{1}{2} \rho V^2 A d \bar{C}_{m_q} \left( \frac{\dot{\theta} d}{V} \right)$$

The analysis presented here requires that the static coefficients,  $C_x$ ,  $C_z$ , and  $C_m$  (which are functions of  $\alpha$ ), be known to a reasonable degree of accuracy. This information can be obtained from static experiments or by approximate theoretical methods. The equations of motion are

$$I \ddot{\theta} = \frac{1}{2} \rho V^2 A d C_m + \frac{1}{2} \rho V^2 A d \bar{C}_{m_q} \left( \frac{\dot{\theta} d}{V} \right) \quad (1)$$

$$m \ddot{X} = -\frac{1}{2} \rho V^2 A C_x \quad (2)$$

$$m \ddot{Z} = -\frac{1}{2} \rho V^2 A C_z + mg \quad (3)$$

$$\bar{V} = \dot{X} \hat{X} + \dot{Z} \hat{Z}$$

$\hat{V} \cdot \hat{X} = \cos(\theta - \alpha)$  and  $\hat{V} \cdot \hat{Z} = \sin(\theta - \alpha)$ . Since  $(\theta - \alpha)$  is very small,  $\hat{V} \cdot \hat{X} \cong 1$  and  $\hat{V} \cdot \hat{Z} \cong (\theta - \alpha)$ . Therefore,

$$\dot{X} = V \quad (4)$$

$$\dot{Z} = -V(\theta - \alpha) \quad (5)$$

### B. Solution Assuming the Vertical Acceleration is Zero ( $\theta = \alpha$ )

Equation (1) is not directly solvable because  $V$  and  $C_m$  are variables. However, when  $C_m$  is a linear function of  $\alpha$ , namely  $C_{m_a} \alpha$ , and the coefficient  $C_x$  is constant,  $C_{x_0}$ , then the independent variable can be changed from time ( $t$ ) to distance ( $X$ ) by employing Eq. (2) and (4) and modified Eq. (1) will then be linear. This transformation is shown below:

$$\dot{\theta} = \frac{d\theta}{dX} \frac{dX}{dt} = \theta' \dot{X}$$

$$\ddot{\theta} = \dot{X}^2 \theta'' + \ddot{X} \theta'$$

But  $\dot{X} = V$ , and

$$\ddot{X} = -\frac{\rho V^2 A}{2m} C_{x_0}$$

Therefore,

$$\dot{\theta} = \theta' V \quad (6)$$

$$\ddot{\theta} = V^2 \theta'' - \frac{\rho V^2 A}{2m} C_{x_0} \theta' \quad (7)$$

<sup>7</sup> See Section II B.

Equation (1) now becomes

$$I \left[ V^2 \theta'' - \frac{\rho V^2 A}{2m} C_{x_0} \theta' \right] = \frac{1}{2} \rho V^2 A d C_{m_a} \theta + \frac{1}{2} \rho V^2 A d^2 \overline{C_{m_q}} \theta'$$

Dividing by  $V^2$  and rearranging,

$$I \theta'' - \frac{\rho A I}{2m} \left[ C_{x_0} + \left( \frac{md^2}{I} \right) \overline{C_{m_q}} \right] \theta' - \frac{\rho A d}{2} C_{m_a} \theta = 0 \quad (8)$$

Equation (8) is a second-order homogeneous differential equation with constant coefficients. For stable models, i.e.,  $C_m < 0$  (which is the only situation being considered), the well-known solution<sup>8</sup> is

$$\theta = \theta_0 e^{-\lambda X} \cos(\omega X + \phi) \quad (9)$$

where

$$-\lambda = \frac{\rho A}{4m} \left[ C_{x_0} + \left( \frac{md^2}{I} \right) \overline{C_{m_q}} \right] \quad (10)$$

$$\omega = \left[ -\frac{\rho A d}{2I} C_{m_a} + \left\{ \frac{\rho A}{4m} \left( C_{x_0} + \left[ \frac{md^2}{I} \right] \overline{C_{m_q}} \right) \right\}^2 \right]^{1/2}$$

Listed below are representative magnitudes of the terms in this equation (Ref. 6):

$$\begin{aligned} \rho &= 1 \times 10^{-4} \text{ slug/ft}^3 & m &= 1 \times 10^{-3} \text{ slug} & \overline{C_{m_q}} &= -0.1 \\ d &= 0.1 \text{ ft} & I &= 2 \times 10^{-7} \text{ slug-ft}^2 & C_{x_0} &= 1.0 \\ A &= 0.01 \text{ ft}^2 & C_{m_a} &= -0.1 \end{aligned}$$

Inserting these values into the above expression, the following is obtained:

$$-\frac{\rho A d}{2I} C_{m_a} = 2.5 \times 10^{-2} \frac{1}{\text{ft}^2} \text{ and } \left\{ \frac{\rho A}{4m} \left( C_{x_0} + \left[ \frac{md^2}{I} \right] \overline{C_{m_q}} \right) \right\}^2 = 1 \times 10^{-6} \frac{1}{\text{ft}^2}$$

<sup>8</sup>If it is assumed, in addition, that the force coefficient in the Z direction is a linear function  $\alpha$ , i.e.,  $C_{z_a} \alpha$ , and the angle-of-attack small such that  $\sin \alpha = \alpha$  and  $\cos \alpha = 1$  then the following linear solution can be obtained:

$$\alpha = \alpha_0 \exp \left\{ \frac{\rho A}{4m} \left[ C_{x_0} - C_{z_a} + \left( \frac{md^2}{I} \right) \overline{C_{m_q}} \right] X \right\} \cos \left( \left\{ -\frac{\rho A d}{2I} C_{m_a} + \left( \frac{\rho A}{4m} \left[ C_{x_0} - C_{z_a} + \left( \frac{md^2}{I} \right) \overline{C_{m_q}} \right] \right)^2 \right\}^{1/2} X + \phi \right)$$

In general,

$$-\frac{\rho A d}{2I} C_{m_a} > > \left\{ \frac{\rho A}{4m} \left( C_{x_0} + \left[ \frac{md^2}{I} \right] \overline{C_{m_q}} \right) \right\}^2$$

and  $\omega \cong \left[ -\frac{\rho A d}{2I} C_{m_a} \right]^{1/2}$  (11)

Since  $C_{x_0}$  is always positive, a convergent  $\theta$  envelope can only be produced by a negative  $\overline{C_{m_q}}$ . The actual effect on the motion by  $C_{x_0}$  is that of reducing the  $V^2$  term and consequently weakening the static restoring moment  $1/2\rho V^2 A d C_m$ . The decrease in  $V$  per cycle is usually in the order of 2 percent or less. From an energy consideration, more energy is converted from potential energy to kinetic energy as the model oscillates from the initial angle to zero (first quarter cycle) than is converted back to potential energy when the model reaches minus the initial angle. In order to balance the energies, the model will oscillate an additional increment  $\delta\theta$ , tending to cause divergent motion.

Equation (11) states that frequency is a function of  $C_m$  for the special case considered. This result can be extended to the general case by considering the physical contribution, on the oscillatory motion, of all the other coefficients, viz,  $C_x$ ,  $\overline{C_{m_q}}$ ,  $C_z$ . As already described,  $C_x$  reduces the potential energy slightly, by reducing  $V^2$ ;  $-\overline{C_{m_q}}$  appears as a friction term in the equations which dissipates a rather small amount of energy, and  $C_z$ , as we shall see later, increases the potential energy slightly if  $\partial C_z / \partial \alpha > 0$ . All these coefficients have a prominent effect upon the amplitude of oscillation but a relatively second-order effect on the oscillatory frequency. The assumption will be made, now, that frequency is a function of  $C_m$  only.

### C. Nonlinear Versus Linear Pitching Moment

In order to solve the general planar case and understand what errors would result by assuming linear aerodynamics, it is necessary to investigate the motion resulting from nonlinear pitching moments and compare this motion with that resulting from linear pitching moments. Neglecting all terms except the pitching moment, and changing the independent variable from time to distance, Eq. (1) can be written

$$I \theta'' = \frac{1}{2} \rho A d C_m \quad (12)$$

$$\theta'' = k_M C_m(\theta)$$

or

$$\theta' \frac{d\theta'}{dX} = k_M C_m(\theta) \frac{d\theta}{dX}$$

and

$$\int \theta' d\theta' = k_M \int C_m(\theta) d\theta + \text{constant} \quad (13)$$

Two cases will be considered: the linear case (case A),  $C_m(\theta) = C_{m_a} \theta$ ; and the nonlinear case (case B), represented by the family of functions  $C_m(\theta) = M_r \sin(r\theta)$ . The segment of the oscillation being investigated is that portion of the motion as the model oscillates from  $\theta = 0$  deg to  $\theta = \theta_0$ , the maximum angle.

#### 1. Case A

$$\frac{\theta'^2}{2} = k_M C_{m_a} \frac{\theta^2}{2} + \text{constant}$$

When  $\theta = \theta_0$ ,  $\theta' = 0$ . Therefore,

$$\frac{d\theta}{dX} = (-k_M C_{m_a})^{1/2} (\theta_0^2 - \theta^2)^{1/2} \quad (14)$$

(ignoring the sign for the present)

and

$$\int_0^{\theta_0} \frac{d\theta}{(\theta_0^2 - \theta^2)^{1/2}} = (-k_M C_{m_a})^{1/2} \int_0^X dX$$

or

$$X = \left( \frac{1}{-k_M C_{m_a}} \right)^{1/2} \sin^{-1} \left( \frac{\theta}{\theta_0} \right) \quad (15)$$

#### 2. Case B

$$a. C_m(\theta) = M_1 \sin \theta; M_1 < 0$$

$$\frac{\theta'^2}{2} = -k_M M_1 \cos \theta + \text{constant}$$

when  $\theta = \theta_0$ ,  $\theta' = 0$ . Therefore,

$$\frac{d\theta}{dX} = (-2 k_M M_1)^{1/2} (\cos \theta - \cos \theta_0)^{1/2}$$

And

$$X = \left( \frac{-1}{2 k_M M_1} \right)^{1/2} \int_0^\theta \frac{d\theta}{(\cos \theta - \cos \theta_0)^{1/2}}$$

This equation can be put into a more usable form by making the following substitutions:

$$\alpha = \sin \frac{\theta_0}{2}$$

$$\sin \frac{\theta}{2} = \alpha \sin \phi$$

Then,

$$d\theta = \frac{2 \left( \alpha^2 - \sin^2 \frac{\theta}{2} \right)^{1/2}}{(1 - \alpha^2 \sin^2 \phi)^{1/2}} d\phi$$

and

$$\int_0^\theta \frac{d\theta}{(\cos \theta - \cos \theta_0)^{1/2}} = \sqrt{2} \int_0^\phi \frac{d\phi}{(1 - \alpha^2 \sin^2 \phi)^{1/2}}$$

The integral on the right is the standard form of an elliptical integral of the first kind; tabulated solutions are readily available (note  $\theta_0 \geq \theta$ ). Therefore,

$$X = \left( \frac{-1}{k_M M_1} \right)^{1/2} \int_0^\phi \frac{d\phi}{(1 - \alpha^2 \sin^2 \phi)^{1/2}}$$

b. The general case,  $C_m(\theta) = M_r \sin(r\theta)$ , has the following solutions:

$$\frac{d\theta}{dX} = \left( \frac{-2 k_M M_r}{r} \right)^{1/2} (\cos[r\theta] - \cos[r\theta_0])^{1/2} \quad (16)$$

$$X = \left( \frac{-1}{k_M M_r r} \right)^{1/2} \int_0^\phi \frac{d\phi}{(1 - \alpha^2 \sin^2 \phi)^{1/2}} \quad (17)$$

where

$$\alpha = \sin \frac{r\theta_0}{2} \text{ and } \sin \frac{r\theta}{2} = \alpha \sin \phi$$

Using the preceding results, the following ratios can be formed:

$$\frac{\theta'_n}{\theta'_i} = \left\{ \left( \frac{2M_r}{r C_{m_a}} \right) \frac{(\cos[r\theta] - \cos[r\theta_0])}{(\theta_0^2 - \theta^2)} \right\}^{1/2} \quad (18)$$

$$\frac{X_l}{X_n} = \left( \frac{M_r r}{C_{m_a}} \right)^{1/2} \frac{\sin^{-1} \left( \frac{\theta}{\theta_0} \right)}{F_\theta} \quad (19)$$

where

$$F_\theta = \int_0^\phi \frac{d\phi}{(1 - \alpha^2 \sin^2 \phi)^{1/2}}$$

As a basis for comparing the linear and nonlinear motions, the distance period of oscillation will be equal for both cases. Therefore, for a quarter cycle, Eq. (19) is

$$1 = \left( \frac{M_r r}{C_{m_a}} \right)^{1/2} \frac{\pi}{2 F_{\theta_\pi}}$$

or

$$\frac{M_r r}{C_{m_a}} = \frac{4 F_{\theta_\pi}^2}{\pi^2} \quad (20)$$

where  $F_{\theta_\pi}$  is the complete elliptical integral. This constant is plotted in Fig. 10 for  $r = 2/3, 1$ , and  $4/3$ .

Physically, this constant designates the sine curve necessary to replace the linear moment by a sine-shaped moment and still maintain the same frequency of oscillation. Assuming that locally  $\theta_n$  is a slight perturbation of  $\theta_i$ , the following approximate angle ratio can be written

$$\frac{\theta_n}{\theta_i} \cong \frac{\sin \left\{ \frac{\pi}{2} \left( \frac{X_l}{X_n} \right) \tau \right\}}{\sin \left\{ \frac{\pi}{2} \tau \right\}}$$

where

$$\tau = \frac{X}{T/4}, \quad \theta_i = \theta_0 \sin \left( \frac{\pi}{2} \tau \right)$$

and  $X_l/X_n$  is obtained from the local  $\theta_i$  and Eq. (19) and (20). Plots of  $\theta'_n/\theta'_i$ ,  $X_l/X_n$ , and  $\theta_n/\theta_i$  for various  $r$ 's and  $\theta_0$ 's are shown in Fig. 11 through 15.

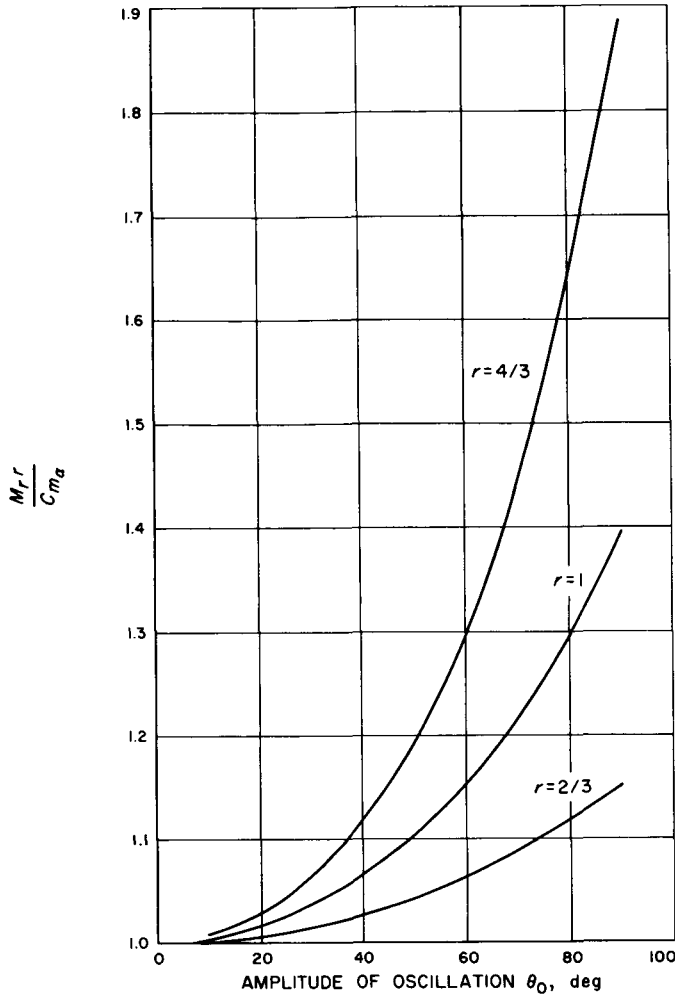


Fig. 10. Ratio of sine designator,  $M,r$ , to linear pitching moment slope vs amplitude of oscillation

These ratios represent errors that would result if a body possessing a sine curve pitching moment were analyzed with a linear pitching moment. At distance  $X$  the linear solution predicts that the model will be at some attitude  $\theta_l$ , but since it is under the influence of a sine curve pitching moment it is actually at angle  $\theta_n$ . Consequently, the aerodynamics acting ( $C_z$ ,  $C_x$ ,  $C_m$ ) are not those for  $\theta_l$ , but are those corresponding to  $\theta_n$ . As an example, consider the model shown in Fig. 1 oscillating a quarter cycle from  $\theta = 0$  deg to  $\theta = 90$  deg while it travels a distance  $X = T/4$ . The aerodynamic coefficients of this body are obtainable from Ref. 5. When the non-linear model has reached the angle  $\theta = 20$  deg, the linear model will be 20 deg divided by  $\theta_n/\theta_l$ . Assuming  $r$  to be about one, the ratio  $\theta_n/\theta_l$  is obtained from Fig. 15, i.e.,  $\theta_n/\theta_l = 1.06$ . Therefore,  $\theta_n = 18.9$  deg. The resultant errors can be determined by comparing the coefficients

for these respective angles. The errors in  $C_N$  and  $C_A$  respectively are 5.5 and 0.4 percent.

The dissipative energy at any instant is proportional to  $C_{m_q}\theta'$ , and for a small portion of the oscillation it is

$$\Delta E = k \overline{C_{m_q}} \theta' \Delta \theta$$

Assuming that  $\theta'_n$  is a small perturbation of  $\theta'_l$  the percentage error resulting from using  $\theta'_l$  can be written

$$\% \Delta E = \frac{\Delta E_n - \Delta E_l}{\Delta E_l} = \frac{(\theta'_n - \theta'_l) \Delta \theta}{\theta'_l \Delta \theta}$$

By extension, the percentage error over a quarter-cycle is

$$\% E = \frac{\int_0^{\theta_0} \left( \frac{\theta'_n}{\theta'_l} - 1 \right) \theta'_l d\theta}{\int_0^{\theta_0} \theta'_l d\theta}$$

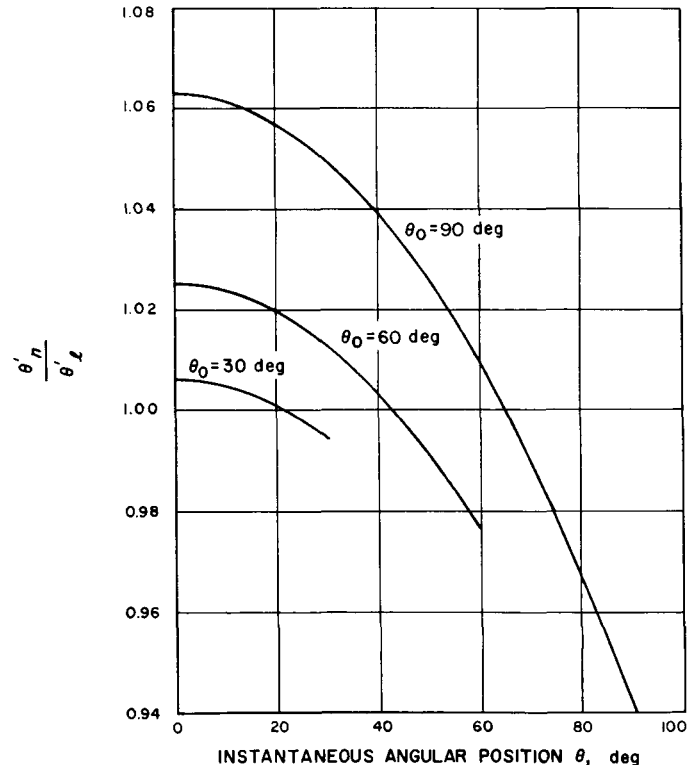


Fig. 11. Ratio of nonlinear to linear angular rates vs the instantaneous angular position for  $r = 1$

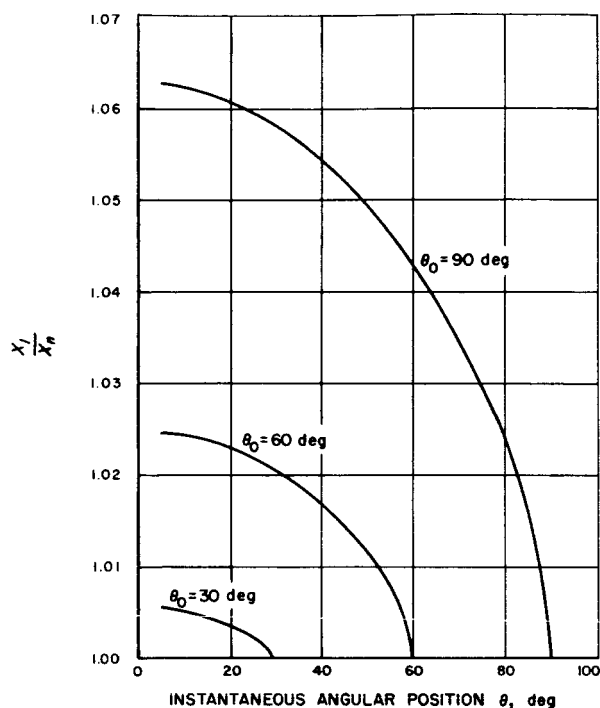


Fig. 12. Ratio of the linear to nonlinear translational position vs the instantaneous angular position for  $r = 1$

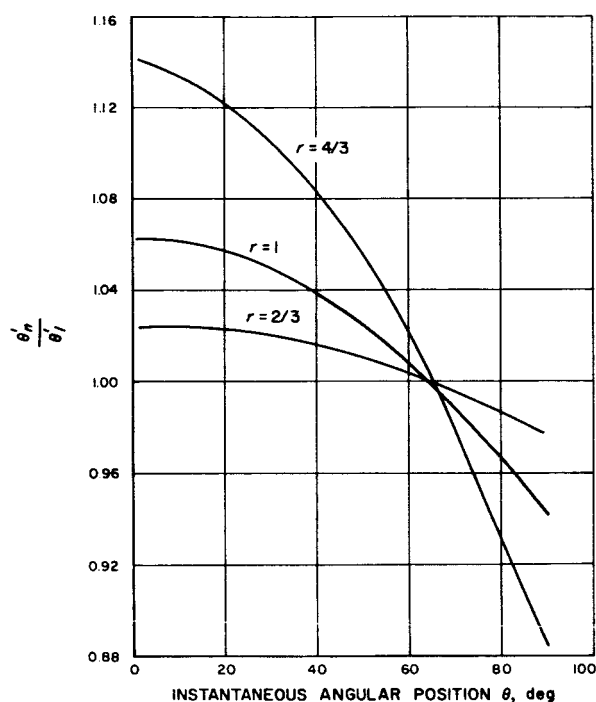


Fig. 13. Ratio of nonlinear to linear angular rates vs the instantaneous angular position for  $\theta_0 = 90$  deg

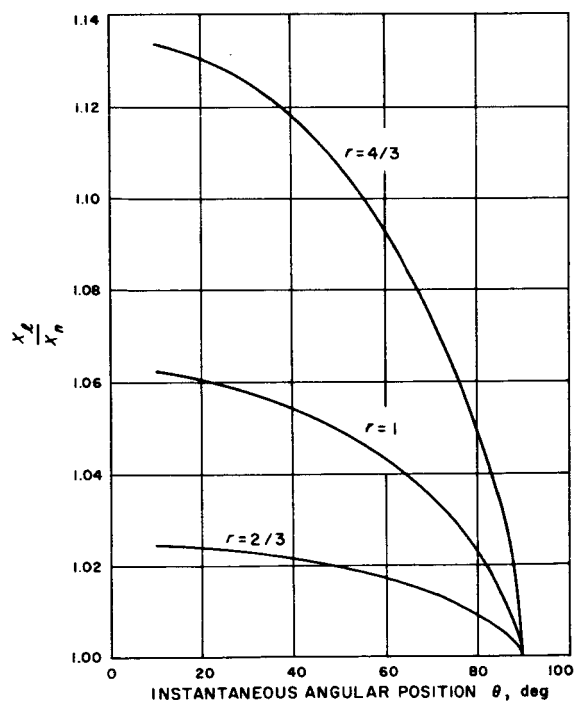


Fig. 14. Ratio of the linear to nonlinear translational position vs the instantaneous position for  $\theta_0 = 90$  deg

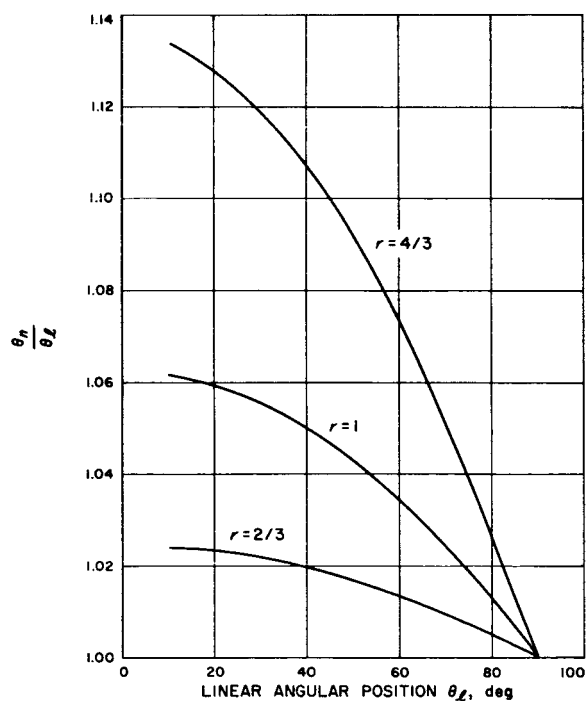


Fig. 15. Ratio of the nonlinear to linear angular position vs the linear angular position for  $\theta_0 = 90$  deg

Employing Eq. (14) and (18), the above error equation reduces to the following:

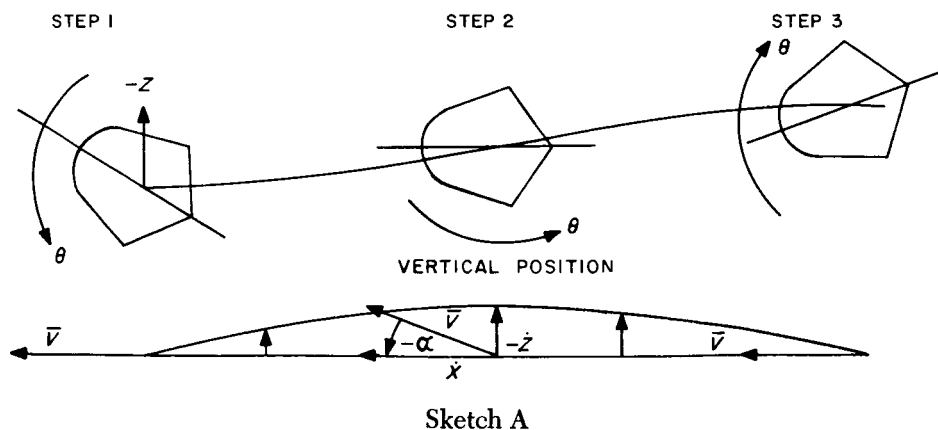
$$\begin{aligned} \% E &= \frac{\int_0^{\theta_0} \left\{ \left[ \left( \frac{2M_r}{r C_{m_a}} \right) (\cos [r\theta] - \cos [r\theta_0]) \right]^{1/2} - (\theta_0^2 - \theta^2)^{1/2} \right\} d\theta}{\int_0^{\theta_0} (\theta_0^2 - \theta^2)^{1/2} d\theta} \\ &= \frac{\left( \frac{2M_r}{r C_{m_a}} \right)^{1/2} \int_0^{\theta_0} \{ \cos [r\theta] - \cos [r\theta_0] \}^{1/2} - \pi/4 \theta_0^2}{\pi/4 \theta_0^2} \end{aligned}$$

As an example, for the case when  $r = 1$  and  $\theta_0 = \pi/2$  the percentage error is about +5 percent. This means that for each quarter cycle of oscillation 5 percent more energy is dissipated with the sine curve pitching moment than the corresponding linear pitching moment. Using the improper pitching moment results in using the wrong instantaneous values of  $\theta$  and  $\theta'$  and, consequently, applying the wrong forces and moments.

The choice of using the sine curve for the nonlinear analysis was not as arbitrary as it might appear. It has been observed that many of the symmetrical configurations have moment curves which can be approximated by sine curves. Figure 16 shows some representative bodies and the corresponding moment curves obtained using the Newtonian Impact Theory (Ref. 6). The plots indicate that the computed pitching moments can be adequately replaced by a sine curve. In order to determine the proper sine curve, it is necessary only to specify a value of  $r$ . From the experimental data,  $\Omega$  is obtained, i.e.,  $\Omega = 2\pi/T$ , where  $T$  is the distance period (ft/cycle).  $C_{m_a}$  is then available from Eq. (11), and  $M_r$  is computed from Eq. (20), or obtained from Fig. 8.

#### D. The Effect of Vertical Motion

Equation (5) indicates that the integral of  $\ddot{Z}$  produces the angle  $(\theta - \alpha)$ . The effect of this small angle on the motion can best be described by sketch A.



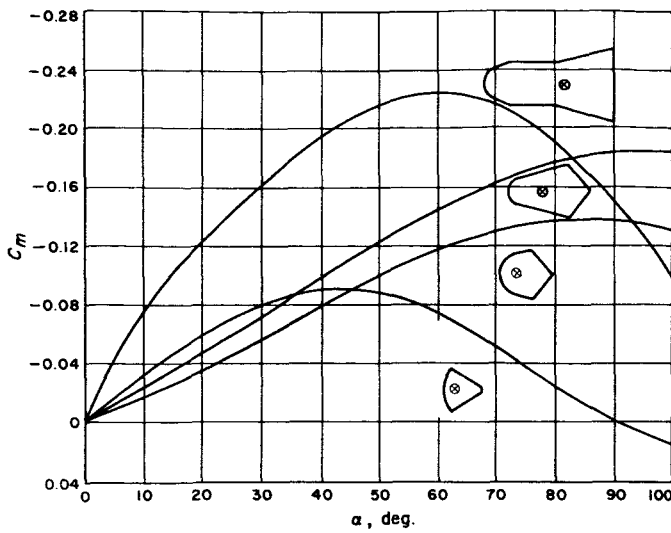


Fig. 16. Pitching moment curves obtained from the Newtonian Impact Theory

A model possessing a  $\partial C_z / \partial \alpha > 0$  is released at step 1 and oscillates to step 2. At the same time, the model is at a positive angle-of-attack and subject to an upward aerodynamic force producing an upward velocity. At step 2, the apparent angle-of-attack is zero; in actuality, it is  $-\alpha$ , as shown. This deviation from the apparent to true angle-of-attack produces a small additional restoring moment which tends to decrease the angle-of-attack envelope. Basically, each instant the potential energy is being increased by an amount proportional to  $(\theta - \alpha)$ .

### 1. Obtaining $(\theta - \alpha)$

The correction resulting from this angle is not the prime contributor to damping, but it must not be ignored. However, reasonable latitude in solving for this angle can be accepted without introducing appreciable errors into the total solution. The following assumptions will be made:

1.  $C_z$  is a function of  $\theta$
2.  $C_m$  is in the form of  $M_r \sin(r\theta)$
3.  $\dot{X}$  is a constant  $\dot{X}_0$

Equation (3) is

$$\ddot{Z} = -\frac{\rho V^2 A}{2m} C_z(\theta) + g \quad (3)$$

But,

$$\dot{Z} = Z' \dot{X}$$

and

$$\ddot{Z} = Z'' \dot{X}^2 + Z' \ddot{X}$$

By the assumption of a constant  $\dot{X}$ ,  $\ddot{X} = 0$  and Eq. (3) now takes the form

$$\frac{dZ'}{dX} = -k_z C_z(\theta) + \frac{g}{\dot{X}_0^2} \quad (3a)$$

where

$$k_z = \frac{\rho A}{2m}$$

By assuming that  $C_m$  is in the form  $M_r \sin(r\theta)$ ,

$$\theta' = \pm \left( k_M \frac{-2M_r}{r} \right)^{1/2} \{ \cos(r\theta) - \cos(r\theta_0) \}^{1/2}$$

During the first half cycle of motion,  $\theta'$  is negative. This can be seen by differentiating Eq. (9). If  $\Omega$  is defined as the experimental angular frequency, then, according to Eq. (11), there must be a linear moment coefficient,  $C_{m_a}$ , such that

$$\Omega^2 = \frac{-\rho A d}{2I} C_{m_a} = -k_M C_{m_a}$$

For the first half cycle,  $\theta'$  can be rewritten as follows:

$$\frac{d\theta}{dX} = -\Omega \left( \frac{2}{r} \frac{M_r}{C_{m_a}} \right)^{1/2} \{ \cos(r\theta) - \cos(r\theta_0) \}^{1/2}$$

Combining this last equation with Eq. (3a),

$$dZ' = \frac{k_z}{\Omega \left( \frac{2}{r} \frac{M_r}{C_{m_a}} \right)^{1/2}} \frac{C_z(\theta) d\theta}{\{ \cos(r\theta) - \cos(r\theta_0) \}^{1/2}} - \frac{\frac{g}{\dot{X}_0^2}}{\Omega \left( \frac{2}{r} \frac{M_r}{C_{m_a}} \right)^{1/2}} \frac{d\theta}{\{ \cos(r\theta) - \cos(r\theta_0) \}^{1/2}}$$

Integrating and noting that  $Z'_0$  is zero, the following result, valid in the first half cycle, is obtained:

$$\begin{aligned}
Z' = & \frac{k_z}{\Omega \left( \frac{2}{r} \frac{M_r}{C_{m_a}} \right)^{1/2}} \int_{\theta_0}^{\theta} \frac{C_z(\theta) d\theta}{\{\cos(r\theta) - \cos(r\theta_0)\}^{1/2}} \\
& - \frac{\frac{g}{\dot{X}_0^2}}{\Omega \left( \frac{2}{r} \frac{M_r}{C_{m_a}} \right)^{1/2}} \int_{\theta_0}^{\theta} \frac{d\theta}{\{\cos(r\theta) - \cos(r\theta_0)\}^{1/2}} \quad (21)
\end{aligned}$$

It should be noted that the last term may also be written  $gX/\dot{X}_0^2$  by a direct integration of Eq. (3a). By changing the independent variable from time to distance, Eq. (5) can be restated as

$$Z' = -(\theta - \alpha) \quad (5a)$$

or

$$\alpha = \theta + Z' \quad (22)$$

### E. General Planar Solution

Restating Eq. (1), with distance as the independent variable:

$$I\theta'' - \frac{I\rho A}{2m} C_x \theta' = \frac{\rho A d}{2} C_m + \frac{\rho A d^2}{2} \overline{C_{m_q}} \theta' \quad (1a)$$

Multiplying through by  $\theta$ ,

$$\theta' \frac{d\theta'}{dX} - \frac{\rho A}{2m} C_x \theta' \frac{d\theta}{dX} = \frac{\rho A d}{2I} C_m \frac{d\theta}{dX} + \frac{\rho A d^2}{2I} \overline{C_{m_q}} \theta' \frac{d\theta}{dX} \quad (23)$$

$C_x$  and  $C_m$  are both functions of  $\alpha$ . However, assuming that  $C_x$  is a direct function of  $\theta$  results in a negligible error. A similar assumption for  $C_m$  will noticeably disrupt the energy balance. Therefore,  $C_m$  will remain a function of  $\alpha$ , i.e., the  $\alpha$  obtained in Eq. (22). Equation (23) now takes the form

$$\left( \frac{md^2}{I} \right) \overline{C_{m_q}} \theta' d\theta = \left( \frac{2m}{\rho A} \right) \theta' d\theta' - \left( \frac{md}{I} \right) C_m(\alpha) d\theta - C_x(\theta) \theta' d\theta$$

And

$$\left( \frac{md^2}{I} \right) \overline{C_{m_q}} \int_{\theta_0}^{\theta} \theta' d\theta = \left( \frac{2m}{\rho A} \right) \int_{\theta'_0}^{\theta'} \theta' d\theta' - \left( \frac{md}{I} \right) \int_{\theta_0}^{\theta} C_m(\alpha) d\theta - \int_{\theta_0}^{\theta} C_x(\theta) \theta' d\theta \quad (24)$$

Integrating over the first half cycle of motion from  $\theta_0$  to  $-(\theta_0 - \delta\theta)$ , Eq. (24) becomes

$$\begin{aligned} \left(\frac{md^2}{I}\right) \overline{C_{m_q}} \int_{\theta_0}^{-(\theta_0 - \delta\theta)} \theta' d\theta &= \left(\frac{2m}{pA}\right) \frac{\theta'^2}{2} \Big|_{\theta'_0}^{-(\theta_0 - \delta\theta)'} \\ &- \left(\frac{md}{I}\right) \int_{\theta_0}^{-(\theta_0 - \delta\theta)} C_m(\alpha) d\theta - \int_{\theta_0}^{-(\theta_0 - \delta\theta)} C_x(\theta) \theta' d\theta \end{aligned}$$

At the peaks,  $\theta_0$  and  $-(\theta_0 - \delta\theta)$ ,  $\theta'$  is zero, therefore,

$$\overline{C_{m_q}} = \frac{-\left(\frac{md}{I}\right) \int_{-(\theta_0 - \delta\theta)}^{\theta_0} C_m(\alpha) d\theta - \int_{-(\theta_0 - \delta\theta)}^{\theta_0} C_x(\theta) \theta' d\theta}{\left(\frac{md^2}{I}\right) \int_{-(\theta_0 - \delta\theta)}^{\theta_0} \theta' d\theta} \quad (25)$$

This general solution can be put into a more useful form if the following assumptions are made:

1.  $C_m(\alpha) = C_m(\theta + Z') \cong C_m(\theta) + \frac{dC_m}{d\theta} Z'$ . Since  $Z'$  is always a small angle, this approximation is quite good.
2.  $\frac{dC_m}{d\theta} = M_r \cos(r\theta)$ . This assumption is based on the premise that  $C_m$  can be replaced by a sine curve,  $M_r \sin(r\theta)$ .
3. And, for the same reason,

$$\theta' = -\Omega [(2/r)(M_r/C_{m_a})]^{1/2} \{\cos(r\theta_0) - \cos(r\theta)\}^{1/2}$$

Note that the assumption  $C_m = M_r \sin(r\theta)$  is only applied to the second order effects  $C_x$ ,  $C_z$ , and  $\overline{C_{m_q}}$ . No restriction is placed on the prime moment function  $C_m(\theta)$ .

Employing these assumptions, the terms in the general solution can be modified.

$$\int_{-(\theta_0 - \delta\theta)}^{\theta_0} C_m(\theta) d\theta = \int_{-\theta_0}^{\theta_0} C_m(\theta) d\theta - \int_{-\theta_0}^{-(\theta_0 - \delta\theta)} C_m(\theta) d\theta$$

Therefore,

$$\int_{-(\theta_0 - \delta\theta)}^{\theta_0} C_m(\alpha) d\theta = \int_{-\theta_0}^{\theta_0} C_m(\theta) d\theta - \int_{-\theta_0}^{-(\theta_0 - \delta\theta)} C_m(\theta) d\theta \\ + M_r \cdot r \int_{-(\theta_0 - \delta\theta)}^{\theta_0} Z' \cos(r\theta) d\theta$$

The first term is zero because of model symmetry. For small  $\delta\theta$ ,  $C_m(\theta)$  can be considered constant, and the second integral reduces to

$$\int_{-\theta_0}^{-(\theta_0 - \delta\theta)} C_m(\theta_0) d\theta \cong -C_m(\theta_0) \cdot \delta\theta$$

Then

$$\int_{-(\theta_0 - \delta\theta)}^{\theta_0} C_m(\alpha) d\theta = C_m(\theta_0) \cdot \delta\theta + M_r \cdot r \int_{-(\theta_0 - \delta\theta)}^{\theta_0} Z' \cos(r\theta) d\theta$$

Inserting the above modifications and the  $\theta'$  assumption, the general equation can be restated in the modified form:

$$\overline{C_{m_q}} = \frac{\left(\frac{rC_{m_a}}{2M_r}\right)^{1/2} \frac{1}{\Omega d} \{C_m(\theta_0) \cdot \delta\theta + M_r \cdot r \int_{-(\theta_0 - \delta\theta)}^{\theta_0} Z' \cos(r\theta) d\theta\} - \int_{-(\theta_0 - \delta\theta)}^{\theta_0} C_x(\theta) \{\cos(r\theta) - \cos(r\theta_0)\}^{1/2} d\theta}{\int_{-(\theta_0 - \delta\theta)}^{\theta_0} \{\cos(r\theta) - \cos(r\theta_0)\}^{1/2} d\theta} \quad (26)$$

Usually,  $\delta\theta < \theta_0$ , and the lower limit can be changed from  $-(\theta_0 - \delta\theta)$  to  $-\theta_0$ .

## F. Applications

The angle-of-attack envelope, and consequently the coefficient of a body possessing linear aerodynamics can be determined exactly from a solution of the linear differential equation of motion (see footnote on page 17). It is desirable to solve the general solution, Eq. (25), assuming linear aerodynamics, and compare it with the exact solution.

The condition of linearity is:

$$C_x = C_{x_0}$$

$$C_z = C_{z_a} \alpha$$

$$C_m = C_{m_a} \alpha$$

From Eq. (3a), ignoring gravity,

$$dZ' = -k_z C_{z_a} \theta dX$$

Over the first half cycle,

$$\theta' = -(k_M C_{m_a})^{1/2} (\theta_0^2 - \theta^2)^{1/2}$$

Therefore,

$$\begin{aligned} Z' &= \frac{-k_Z}{(-k_M C_{m_a})^{1/2}} \int_{\theta_0}^{\theta} \frac{C_{z_a} \theta d\theta}{(\theta_0^2 - \theta^2)^{1/2}} \\ &= \frac{k_Z}{(-k_M C_{m_a})^{1/2}} C_{z_a} (\theta_0^2 - \theta^2)^{1/2} \end{aligned}$$

Inserting  $C_{x_0}$ ,  $C_{m_a}$ ,  $\theta'$ , and  $Z'$  into Eq. (25), it becomes

$$\begin{aligned} \bar{C}_{m_q} = & \frac{-\left(\frac{md}{I}\right) \int_{-(\theta_0 - \delta\theta)}^{\theta_0} \theta d\theta - \left(\frac{md}{I}\right) \frac{k_Z}{(-k_M C_{m_a})^{1/2}} C_{m_a} C_{z_a} \int_{-(\theta_0 - \delta\theta)}^{\theta_0} (\theta_0^2 - \theta^2)^{1/2} d\theta + (-k_M C_{m_a})^{1/2} C_{x_0} \int_{-(\theta_0 - \delta\theta)}^{\theta_0} (\theta_0^2 - \theta^2)^{1/2} d\theta}{- \left(\frac{md^2}{I}\right) (-k_M C_{m_a})^{1/2} \int_{-(\theta_0 - \delta\theta)}^{\theta_0} (\theta_0^2 - \theta^2)^{1/2} d\theta} \end{aligned}$$

$$1. \int_{-(\theta_0 - \delta\theta)}^{\theta_0} \theta d\theta = \frac{\theta_0^2}{2} - \frac{1}{2} (\theta_0^2 - 2\theta_0 \delta\theta + \delta\theta^2) \cong \theta_0 \delta\theta$$

$$2. \left(\frac{md}{I}\right) \frac{k_Z C_{m_a}}{(-k_M C_{m_a})^{1/2}} = (-k_M C_{m_a})^{1/2}$$

3. Assuming that  $\delta\theta < \theta_0$ ,

$$\int_{-(\theta_0 - \delta\theta)}^{\theta_0} (\theta_0^2 - \theta^2)^{1/2} d\theta = \theta_0^2 \frac{\pi}{2}$$

Combining the above,

$$\bar{C}_{m_q} = \frac{\frac{\delta\theta}{\theta_0} \frac{2}{\pi} \frac{C_{m_a}}{(-k_M C_{m_a})^{1/2}} + C_{z_a} - C_{x_0}}{\left(\frac{md^2}{I}\right)}$$

The linear solution is

$$\alpha = \alpha_0 \exp \left\{ \frac{k_Z}{2} \left[ C_{x_0} - \dot{C}_{z_a} + \left(\frac{md^2}{I}\right) \bar{C}_{m_q} \right] X \right\} \cos \left( \left\{ -k_M C_{m_a} + \left(\frac{k_Z}{2} \left[ C_{x_0} - C_{z_a} + \left(\frac{md^2}{I}\right) \bar{C}_{m_q} \right] \right)^2 \right\} X + \phi \right)$$

From this equation the damping coefficient is

$$\overline{C_{m_q}} = \frac{\frac{2}{k_z \cdot X} \ln \left( \frac{\alpha}{\alpha_0} \right) + C_{z_a} - C_{x_0}}{\left( \frac{md^2}{I} \right)}$$

1. At the first half cycle,

$$X = \frac{\pi}{(-k_M C_{m_a})^{1/2}}$$

$$2. \quad \frac{2}{k_z \cdot X} = \frac{-2md}{\pi I} \frac{C_{m_a}}{(-k_M C_{m_a})^{1/2}}$$

3. Expanding  $\ln \left( \frac{\alpha}{\alpha_0} \right)$  is a series,

$$\ln \left( \frac{\alpha}{\alpha_0} \right) = -\frac{\delta\alpha}{\alpha_0} - \frac{1}{2} \left( \frac{\delta\alpha}{\alpha_0} \right)^2 - \frac{1}{3} \left( \frac{\delta\alpha}{\alpha_0} \right)^3 + \dots$$

For a body such as a cone the decay rate,  $\delta\alpha/\alpha_0$ , is in the order of 0.05, whereas for the blunter bodies it will be closer to 0.02. If only the first term in the series is used, these decay rates correspond to errors of 2 and 1 percent, respectively.

Combining the above and substituting  $-\frac{\delta\alpha}{\alpha_0}$  for  $\ln \left( \frac{\alpha}{\alpha_0} \right)$  the following solution for  $\overline{C_{m_q}}$  is obtained:

$$\overline{C_{m_q}} = \frac{\frac{\delta\alpha}{\alpha_0} \frac{2}{\pi} \frac{C_{m_a}}{(-k_M C_{m_a})^{1/2}} + C_{z_a} - C_{x_0}}{\left( \frac{md^2}{I} \right)}$$

Since  $\frac{\delta\alpha}{\alpha_0}$  is almost identical to  $\frac{\delta\theta}{\theta_0}$ , it follows that the two approaches yield almost identical results.

Generally, the aerodynamic coefficients are not linear, and numerical integrations are required to solve the terms of Eq. (26). However, for the purpose of demonstrating the technique, an example has been chosen which lends itself to the more conventional integration methods, and yet is representative of nonlinear motion. Consider a configuration whose aerodynamic coefficients are described by the following equations:

$$C_A = A \cos \alpha$$

$$C_N = N \sin \alpha$$

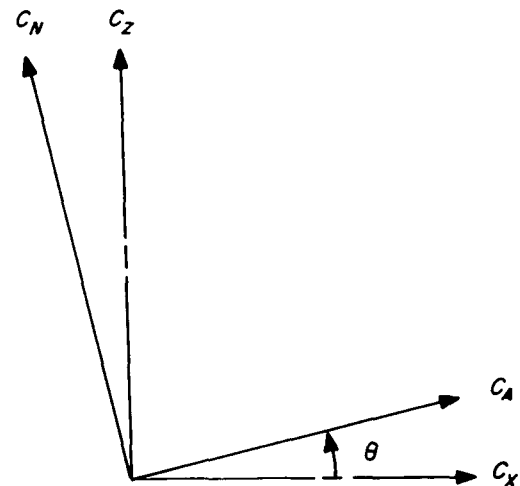
$$C_M = M \sin \alpha$$

(This set of coefficients corresponds favorably to the model in Fig. 1.) The body is released at  $\theta_0 = \pi/2$ , and after a half cycle the motion has decayed an amount  $\delta\theta$  ( $\delta\theta < \pi/2$ ). During the half cycle, the body has traveled, with respect to the air flow, a distance  $T/2$ .

## 1. Preliminaries

$$a. \quad \Omega = \frac{2\pi}{T}$$

- b. The ratio  $M/C_{m_a}$  is obtained from Fig. 10 using the parameters  $r = 1$  and  $\theta_0 = 90$  deg.



Sketch B

$$C_Z = C_N \cos \theta - C_A \sin \theta$$

$$= N \sin \theta \cos \theta - A \cos \theta \sin \theta$$

$$= (N - A) \sin \theta \cos \theta$$

$$C_X = C_N \sin \theta + C_A \cos \theta$$

$$= N \sin^2 \theta + A \cos^2 \theta = N - (N - A) \cos^2 \theta$$

## 2. Obtaining $Z'$

The effect of gravity will be neglected in this solution.  $Z'$  is obtained from Eq. (21) and the above information as follows:

$$Z' = \frac{k_z}{\Omega \left( 2 \frac{M}{C_{m_a}} \right)^{1/2}} \int_{\theta_0}^{\theta} \frac{C_z(\theta) d\theta}{\cos^{1/2} \theta} = \frac{k_z (N - A)}{\Omega \left( 2 \frac{M}{C_{m_a}} \right)^{1/2}} \int_{\pi/2}^{\theta} \sin \theta \cos^{1/2} \theta d\theta$$

Upon evaluating the integral,

$$Z' = \frac{-k_z (N - A)}{\Omega \left( 2 \frac{M}{C_{m_a}} \right)^{1/2}} \frac{2}{3} \cos^{3/2} \theta$$

### 3. Obtaining $\overline{C_{m_q}}$ :

The modified solution is

$$\overline{C_{m_q}} = \frac{\left( \frac{C_{m_a}}{2M} \right)^{1/2} \frac{1}{\Omega d} \left\{ C_m(\pi/2) \cdot \delta \theta + M \int_{-\pi/2}^{\pi/2} Z' \cos \theta d\theta \right\} - \left( \frac{1}{md^2} \right) \int_{-\pi/2}^{\pi/2} C_x(\theta) \cos^{1/2} \theta d\theta}{\int_{-\pi/2}^{\pi/2} \cos^{1/2} \theta d\theta}$$

$$\text{a.} \quad \int_{-\pi/2}^{\pi/2} Z' \cos \theta d\theta = - \frac{2k_z (N - A)}{3\Omega \left( 2 \frac{M}{C_{m_a}} \right)^{1/2}} \int_{-\pi/2}^{\pi/2} \cos^{5/2} \theta d\theta$$

but

$$\int_{-\pi/2}^{\pi/2} \cos^{5/2} \theta d\theta = \frac{2}{5} \cos^{3/2} \theta \sin \theta \Big|_{-\pi/2}^{\pi/2} + \frac{3}{5} \int_{-\pi/2}^{\pi/2} \cos^{1/2} \theta d\theta$$

therefore,

$$\int_{-\pi/2}^{\pi/2} Z' \cos \theta d\theta = - \frac{2}{5} \frac{k_z (N - A)}{\Omega \left( 2 \frac{M}{C_{m_a}} \right)^{1/2}} \int_{-\pi/2}^{\pi/2} \cos^{1/2} \theta d\theta$$

b.

$$\begin{aligned}
\int_{-\pi/2}^{\pi/2} C_X(\theta) \cos^{1/2} \theta d\theta &= \int_{-\pi/2}^{\pi/2} \{N - (N - A) \cos^2 \theta\} \cos^{1/2} \theta d\theta \\
&= N \int_{-\pi/2}^{\pi/2} \cos^{1/2} \theta d\theta - \frac{3(N - A)}{5} \int_{-\pi/2}^{\pi/2} \cos^{1/2} \theta d\theta \\
&= \frac{2N + 3A}{5} \int_{-\pi/2}^{\pi/2} \cos^{1/2} \theta d\theta
\end{aligned}$$

c. It can be shown that

$$\int_{-\pi/2}^{\pi/2} \cos^{1/2} \theta d\theta = -\frac{4}{\sqrt{2}} \int_0^{\pi/2} \frac{d\phi}{\left(1 - \frac{1}{2} \sin^2 \phi\right)^{1/2}} + \frac{8}{\sqrt{2}} \int_0^{\pi/2} \left(1 - \frac{1}{2} \sin^2 \phi\right)^{1/2} d\phi$$

The solution contains complete elliptical integrals of the first and second kind.

Combining the terms, the final solution for  $\overline{C_{m_q}}$  is

$$\overline{C_{m_q}} = \left(\frac{C_{m_a}}{2M}\right)^{1/2} \frac{1}{\Omega d} \left\{ \frac{C_m(\theta_0)}{E} \delta\theta - \frac{2k_z(N - A)}{5\Omega \left(2 \frac{M}{C_{m_a}}\right)^{1/2}} M \right\} - \left(\frac{I}{md^2}\right) \left(\frac{2N + 3A}{5}\right) \quad (27)$$

where

$$E = \int_{-\pi/2}^{\pi/2} \cos^{1/2} \theta d\theta$$

#### 4. Numerical Solution

In order to verify that Eq. (27) is correct, a hypothetical case was formulated and its motion calculated by the computer motion program. Below are lists of the computer inputs and the predicted decay and frequency. The computed motion is shown in Fig. 17.

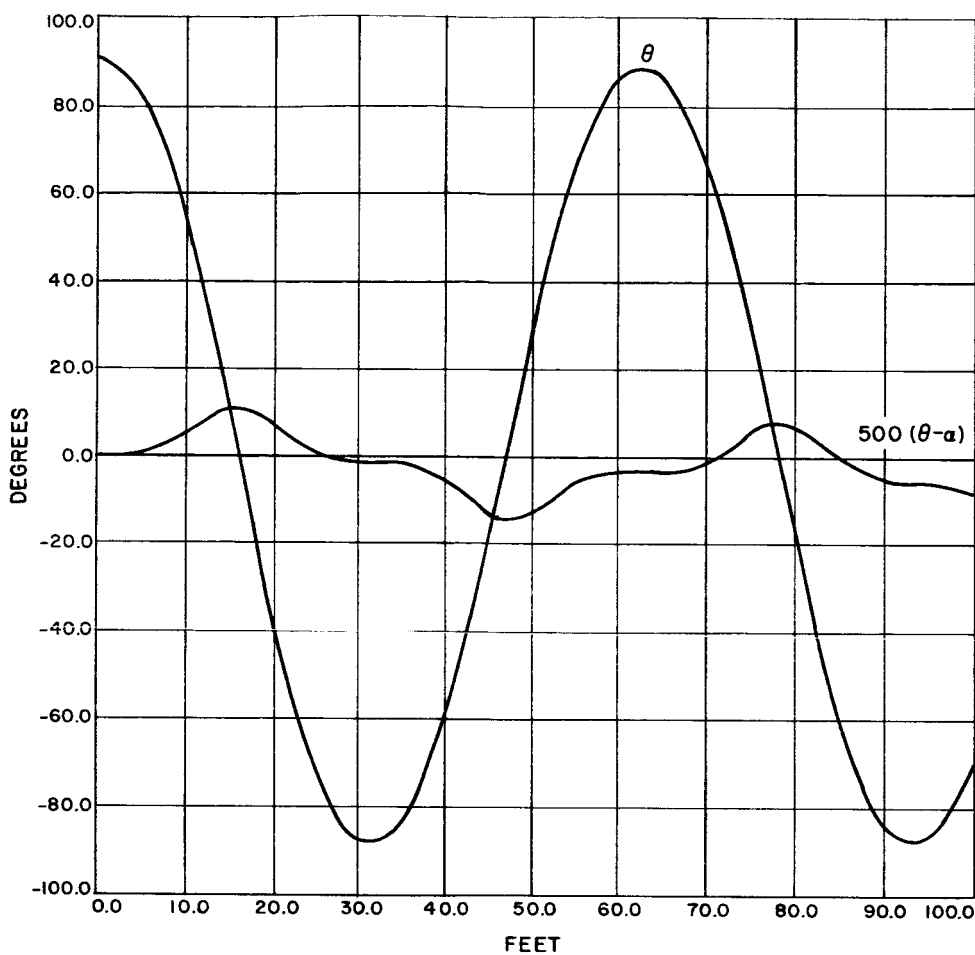


Fig. 17. Computer motion for hypothetical numerical solution

a. Inputs

Aerodynamic coefficients:

$$C_A = 0.7 \cos \alpha$$

$$C_N = 1.1 \sin \alpha$$

$$C_m = -0.18 \sin \alpha$$

$$\overline{C_{m_q}} = -0.1$$

Constants:

$$I_2 = 1.8 \times 10^{-7} \text{ slug-ft}^2$$

$$m = 7.0 \times 10^{-4} \text{ slug}$$

$$d = 8.0 \times 10^{-2} \text{ ft}$$

$$\rho = 7.0 \times 10^{-5} \text{ slug/ft}^3$$

Initial conditions:

$$\dot{X}_0 = 4.0 \times 10^3 \text{ ft/sec}$$

$$\theta_0 = \pi/2$$

b. Outputs

$$\delta\theta = 0.695 \text{ deg} \equiv 1.213 \times 10^{-2} \text{ rad}$$

$$\Omega = 0.10062 \text{ rad/ft}$$

Using the computer inputs and results, Eq. (27) was solved:  $M/C_{m_a}$  is obtained from Eq. (20), for  $r = 1$ ,  $\frac{M}{C_{m_a}} = 1.393$

Experimentally,  $\Omega = 0.10062 \text{ rad/ft}$ ; from Eq. (11),  $\Omega^2 = k_M C_{m_a}$ .

$$k_M = \frac{\rho A d}{2I} = \frac{(7.0 \times 10^{-5}) (8.0 \times 10^{-2})^3 \pi/4}{2(1.8 \times 10^{-7}) \text{ ft}^2} = 0.07819 \frac{1}{\text{ft}^2}$$

$$C_{m_a} = \frac{\left(0.10062 \cdot \frac{1}{\text{ft}}\right)^2}{0.07819 \frac{1}{\text{ft}^2}} = -0.1296$$

Using this ratio for  $M/C_{m_a}$ ,  $M = -0.1805$ . The value of  $M$  used in the computer analysis was  $-0.1800$ . This 0.25 percent deviation is primarily due to the second-order effects and slightly due to the small intrinsic error of a computer operation. To duplicate the reduction of actual free-flight data, the value  $M = -0.1805$  will be used.

Eq. (27) is:

$$\overline{C_{m_a}} = \left(\frac{C_{m_a}}{2M}\right)^{1/2} \frac{1}{\Omega d} \left[ \frac{M}{E} \delta\theta - \frac{2k_z(N-A)}{5\Omega \left(2\frac{M}{C_{m_a}}\right)^{1/2}} M \right] - \left(\frac{I}{md^2}\right) \left(\frac{2N+3A}{5}\right)$$

$$E = -\frac{4}{\sqrt{2}} \int_0^{\pi/2} \frac{d\phi}{\left(1 - \frac{1}{2} \sin^2 \phi\right)^{1/2}} + \frac{8}{\sqrt{2}} \int_0^{\pi/2} \left(1 - \frac{1}{2} \sin^2 \phi\right)^{1/2} d\phi$$

$$= -\frac{4}{\sqrt{2}} (1.8541) + \frac{8}{\sqrt{2}} (1.3506) = 2.396$$

$$k_z = \frac{\rho A}{2m} = \frac{(7.0 \times 10^{-5}) (8.0 \times 10^{-2})^2 \pi/4}{2(7.0 \times 10^{-4})} \frac{1}{\text{ft}} = 2.513 \times 10^{-4} \frac{1}{\text{ft}}$$

$$\left( \frac{2M}{C_{m_a}} \right)^{1/2} = (2 \times 1.393)^{1/2} = 1.669$$

$$\left\{ \frac{M}{E} \delta\theta - \frac{2k_z(N-A)}{5\Omega \left( \frac{2M}{C_{m_a}} \right)^{1/2}} M \right\} = \left\{ \frac{-0.1805}{2.396} (1.213 \times 10^{-2}) + \frac{2(2.513 \times 10^{-4}) (0.4) (0.1805)}{5(0.1006) (1.669)} \right\}$$

$$= \{-0.09136 \times 10^{-2} + 0.00432 \times 10^{-2}\} = -8.704 \times 10^{-2}$$

$$\overline{C_{m_q}} = \frac{10^2}{(1.669) (0.1006) (8.0)} (-0.08704 \times 10^{-4})$$

$$- \frac{(1.8 \times 10^{-7})}{(7.0 \times 10^{-4}) (8.0 \times 10^{-2})^2} \left( \frac{2.2 + 2.1}{5} \right)$$

$$\overline{C_{m_q}} = -0.0648 - 0.0346 = -0.0994$$

Since the input value was  $-0.1000$ , this is an error of 0.6 percent. Most of this error is the result of neglecting gravity. A superficial verification of this is obtained by evaluating  $Z'$  at its maximum value when  $\theta = 0$  deg. Neglecting gravity,  $Z' = 0.0228$  deg; including gravity  $Z' = 0.0210$  deg, which is a decrease of 10 percent. Since the  $Z'$  term reduces the solution of  $\overline{C_{m_q}}$  about 5 percent, the gravity term<sup>9</sup> will increase the final value approximately 0.5 percent and reduce the small error even further.

This high accuracy may be due to the fact that the example problem corresponded exactly to the assumption made in the derivation of the general equation, namely, that  $C_m = M \sin \theta$ . To discount this argument, the following cases were considered: the original moment curve

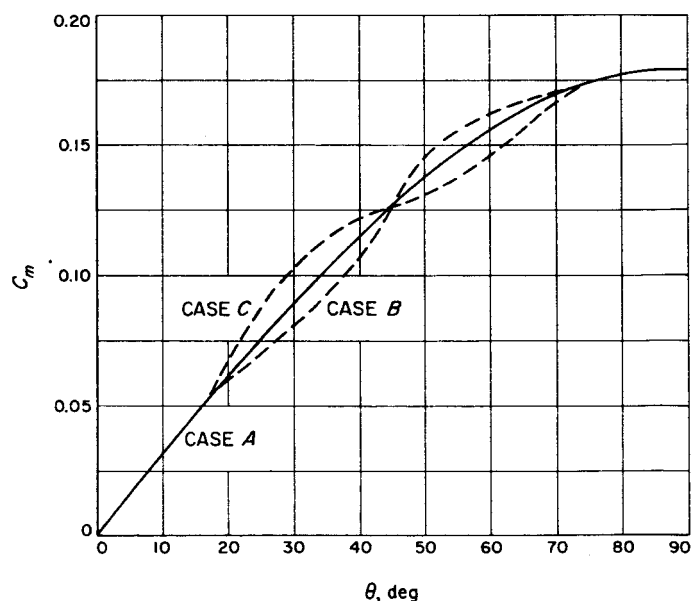


Fig. 18. Perturbated moment curve

<sup>9</sup>The gravity term is obtained from  $Z'_g = (gX/\dot{X}_0^2)$ , where  $X$  was obtained from the computer output. This  $Z'$  value at  $\theta = 0$  agrees exactly with the computer results.

(curve A) was perturbed into curves B and C as shown in Fig. 18. There is no consistent pattern relating the three curves except that the area under each curve is about the same, and the index  $r$  is 1 in each case. Holding all else constant, the motion was computed for curves B and C, and the  $\overline{C_{m_q}}$ 's were calculated for each case from Eq. (27).

The respective decays per half cycle,  $\overline{C_{m_q}}$ 's, and errors are listed as follows:

Case	Decay, deg	$\overline{C_{m_q}}$	Error (including a $-0.5$ percent shift due to gravity), %
A	0.695	$-0.0994$	0.1
B	0.715	$-0.1014$	$-1.9$
C	0.707	$-0.1003$	$-0.8$

## V. CONCLUSION

The determination of the dynamic damping parameter  $C_{m_q}$ , from wind-tunnel free-flight data, requires an accurate solution of the equations for the model attitude during flight. A basic premise employed in formulating the solution presented is that all forces, except the damping force, are known. For purposes of analysis, the free-flight motion is separated into two categories: planar motion, resulting from a smooth release and mass symmetry, and nonplanar motion, due to some sort of anomaly. The latter situation can be handled with the general motion computer program. However, the reiterative process involved could become rather costly and time consuming and should be avoided. Models demonstrating planar motion can be analyzed with the equations developed herein. These equations were formulated on the premise that the instantaneous frequency of oscillation is essentially a function of the pitching moment; and, that this frequency is obtained by assuming that the nonlinear moment can be represented by a sine curve. Similar analyses could be performed with other nonlinear moment curves such as a power series representation. A sine curve was chosen here because it adequately represents a large number of configurations as indicated in Fig. 16, and also because it lends itself well to analysis.

The examples demonstrate the validity of the approach. The first example considers linear aerodynamics; the superb correlation between the solution using the devel-

oped equations and the exact solution of the differential equation verify the correctness of the formulation. The second example considers nonlinear aerodynamics. The numerical solutions of the nonlinear problem considered demonstrate the validity of this approach and indicate, as expected, that solution accuracy decreases as the actual pitching moment curve deviates from a sine curve. It appears, however, that the effect of deviations in the  $C_m$  curve is noticeably attenuated in the final result, and the total accuracy is still quite high (even when the deviation is substantial). It is expected that this solution will, in general, yield results accurate to within  $\pm 5$  percent.

The solution offers the additional advantage of providing a basis for interpreting the relative importance of each of the parameters. For instance, in the numerical solution of the second example (Case A), the Z term contributed about 5 percent to the solution,  $C_x$  about 35 percent, and  $\delta\theta$  about 60 percent. If another body of not too dissimilar aerodynamics exhibits a  $\delta\theta$  twice as great, certainly a good approximation to the solution could be obtained from just using the  $\delta\theta \cdot C_m(\theta_0)$  term. Also, by replacing  $C_z$  with an approximate equation, its approximate effect on the total solution could be determined. If it is small, this approximate solution will be all that is necessary. It is conceivable that solutions for families of  $C_x$ 's and  $C_z$ 's can be obtained and serve as a guide, if not the complete solution, for an arbitrary planar case.

## NOMENCLATURE

- $A$  reference area corresponding to maximum body diameter,  $d$
- c.m. distance from the nose of the model to the center-of-mass
- c.p. distance from the nose of the model to the aerodynamic center-of-pressure
- $\bar{C}_{m_q}$  dynamic damping parameter,
- effective constant value of  $\left\{ \left[ \frac{\partial C_m}{\partial \left( \frac{\dot{\theta} d}{V} \right)} \right]_{\dot{\theta} \rightarrow 0} + \left[ \frac{\partial C_m}{\partial \left( \frac{\dot{a} d}{V} \right)} \right]_{\dot{a} \rightarrow 0} \right\}$
- $C_{m_a}$  linear pitching moment slope, per radian
- $C_{x_0}$  aerodynamic coefficient in the  $X$  direction at zero angle of attack
- $C_{( )}$  dimensionless aerodynamic coefficient; subscripts are as follows:  
 $A$ , axial force, acts along body axis;  $N$ , normal force, acts normal to the body;  $X$ , acts parallel to the inertial  $X$  and opposite in direction;  $Z$ , acts parallel to the inertial  $Z$  and opposite in direction;  $m$ , pitching moment
- $d$  reference length — maximum body diameter
- $e_1, e_2, e_3$  an orthogonal body axes system fixed at the center-of-mass
- $F_\theta \int_0^\phi \frac{d\phi}{(1 - \alpha^2 \sin^2 \phi)^{1/2}}$
- $F_1, F_2, F_3$  aerodynamic forces along axes  $e_1, e_2, e_3$
- $g$  gravitational acceleration
- $I$  moment of inertia about the  $Y$  axis
- $I_1, I_2, I_3$  principal moments of inertia along axes  $e_1, e_2, e_3$
- $k_x \frac{\rho A d}{2I}$
- $k_z \frac{\rho A}{2m}$
- $m$  mass of model
- $M_r$  maximum value of the sine curve pitching moment of index  $r$
- $M_1, M_2, M_3$  aerodynamic moments along axes  $e_1, e_2, e_3$
- $n$  computer integration index number
- $N$  maximum  $n$
- $q$  dynamic pressure,  $\frac{1}{2} \rho V^2$ ;  $q_c$  is based upon  $V_c$
- $r$  index denoting the angular position when maximum pitching moment occurs.

## NOMENCLATURE (Cont'd)

- $\bar{r}$  vector from the center-of-mass to the geometric centroid (see Fig. 5)  
 $t$  time  
 $\delta t$  computer integration time interval; also small interval of time  
 $T$  distance period of oscillation, ft/cycle  
 $u_1, u_2, u_3$  components of velocity along  $e_1, e_2, e_3$  at the center-of-mass  
 $v_1, v_2, v_3$  components of velocity along  $e_1, e_2, e_3$  at the geometric centroid (see Fig. 5)  
 $V$  velocity of model at the center-of-mass  
 $V_c$  velocity of model at geometric centroid (see Fig. 5)  
 $V_\infty$  free stream velocity, i.e., the steady flow in the wind tunnel  
 $\bar{V}_\infty = V_\infty \hat{X}$   
 $\tilde{X}, \tilde{Y}, \tilde{Z}$  an axes system parallel to  $X_T, Y_T, Z_T$  but fixed to the medium (see Fig. 3)  
 $X_m, Y_m, Z_m$  an axes system parallel to  $\tilde{X}_T, \tilde{Y}_T, \tilde{Z}_T$  fixed at the model center-of-mass (see Fig. 3)  
 $\tilde{X}_T, \tilde{Y}_T, \tilde{Z}_T$  wind tunnel fixed Cartesian axes system, assumed to be an inertial system (see Fig. 3)  
 $\alpha$  angle-of-attack in the vertical plane,  $\tan^{-1} \frac{v_3}{v_1}$   
 $\beta$  angle of slide-slip,  $\tan^{-1} \frac{v_2}{v_1}$   
 $\eta$  total angle of attack,  $\tan^{-1} \frac{\sqrt{v_2^2 + v_3^2}}{v_1}$   
 $\delta\theta$  angular decay per half cycle  
 $\rho$  atmospheric density  
 $\psi, \theta, \phi$  Euler angles (see Fig. 4)  
 $\omega$  oscillatory frequency used in Eq. (11), rad/ft  
 $\bar{\omega}$  angular velocity of the model with respect to inertial space with components  $\omega_1, \omega_2$ , and  $\omega_3$  along the  $e_1, e_2, e_3$  axes  
 $\Omega$  oscillatory frequency obtained experimentally, rad/ft  
 $(\dot{\phantom{x}})(\ddot{\phantom{x}})$  first and second derivatives of  $(\phantom{x})$  with respect to time  
 $(\dot{\phantom{x}})'(\ddot{\phantom{x}})''$  first and second derivatives of  $(\phantom{x})$  with respect to  $X$   
 $(\bar{\phantom{x}})$  vector; also, the effective term  $\bar{C}_{m_q}$   
 $(\hat{\phantom{x}})$  unit vector in the  $(\phantom{x})$  direction

## NOMENCLATURE (Cont'd)

### Subscripts

- $l$  linear
- $n$  nonlinear
- $o$  initial conditions

## REFERENCES

1. Tobak, Murray, and Wehrend, William R., Jr., *Stability Derivatives of Cones at Supersonic Speeds*, NACA TN 3788, September, 1956.
2. Allen, Julian H., *Motion of a Ballistic Missile Angularly Misaligned with the Flight Path Upon Entering the Atmosphere and Its Effect Upon Aerodynamic Heating, Aerodynamic Loads, and Missile Distance*, NACA TN 4048, October, 1957.
3. Dayman, Bain, Jr., Brayshaw, James M., Nelson, Duane A., Jaffe, Peter, and Babineaux, Terry L., *The Influence of Shape on Aerodynamic Damping of Oscillatory Motion During Mars Atmosphere Entry and Measurement of Pitch Damping at Large Oscillation Amplitudes*, Technical Report No. 32-380, Jet Propulsion Laboratory, Pasadena, February, 1963.
4. Dayman, Bain, Jr., *Simplified Free-Flight Testing in a Conventional Wind Tunnel*, Technical Report No. 32-346, Jet Propulsion Laboratory, Pasadena, October, 1962.
5. Peterson, Victor L., *Motion of a Short 10-deg Blunted Cone Entering a Martian Atmosphere at Arbitrary Angles of Attack and Arbitrary Pitching Rates*, NASA TN D-1326, May, 1962.
6. Truit, Robert W., *Hypersonic Aerodynamics*, Ronald Press, 1959, pp. 4-13.